AD-A193 894 SURFACE-WAVE MODEL UNCERTAINTY ASSESSMENT(U) NAVAL OCEAN SYSTEMS CENTER SAN DIEGO CA T N ROY ET AL. 1/1
NOV 87 NOSC-TR-1199

UNCLASSIFIED F/G 20/14 NL

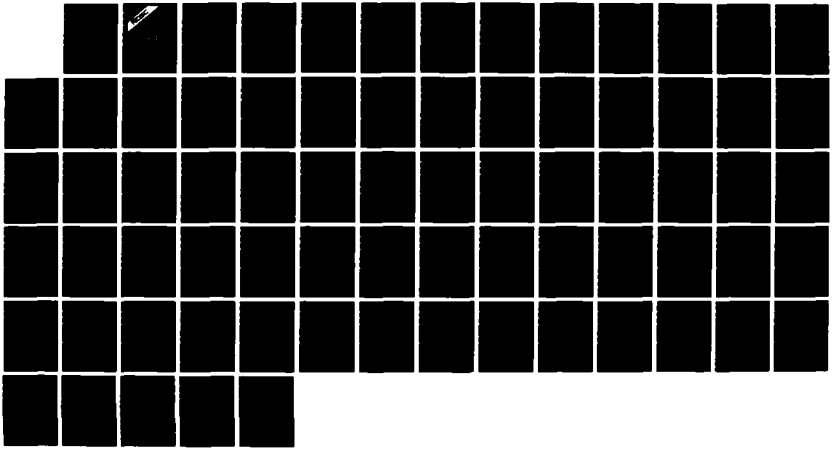

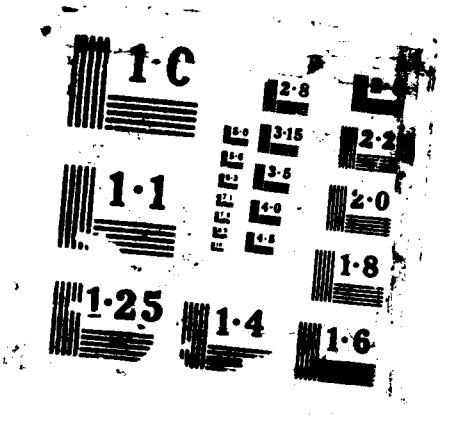
1·C
1·1
1·25
1·4
2·8
3·15
3·5
2·2
2·0
1·8
1·6

NAVAL OCEAN SYSTEMS CENTER San Diego, California 92152-5000

Technical Report 1199
November 1987

Surface-Wave Model Uncertainty Assessment

T. N. Roy
D. B. Sailors
W. K. Moision

NAVAL OCEAN SYSTEMS CENTER

San Diego, California 92152-5000

E. G. SCHWEIZER, CAPT, USN
Commander

R. M. HILLYER
Technical Director

ADMINISTRATIVE INFORMATION

The work reported herein was performed by members of the Ionospheric Branch, Ocean and Atmospheric Sciences Division, Naval Ocean Systems Center, during the period October 1984 through September 1986. The project was sponsored by Space and Naval Warfare Systems Command.

Released by
D.B. Sailors, Head
Ionospheric Branch

Under authority of
J.H. Richter, Head
Ocean and Atmospheric
Sciences Division

REPORT DOCUMENTATION PAGE

1a. REPORT SECURITY CLASSIFICATION UNCLASSIFIED	1b. RESTRICTIVE MARKINGS
2a. SECURITY CLASSIFICATION AUTHORITY	3. DISTRIBUTION/AVAILABILITY OF REPORT
2b. DECLASSIFICATION/DOWNGRADING SCHEDULE	
4. PERFORMING ORGANIZATION REPORT NUMBER(S) NOSC TR 1199	5. MONITORING ORGANIZATION REPORT NUMBER(S)
6a. NAME OF PERFORMING ORGANIZATION Naval Ocean Systems Center 6b. OFFICE SYMBOL (if applicable) NOSC	7a. NAME OF MONITORING ORGANIZATION
6c. ADDRESS (City, State and ZIP Code) San Diego, CA 92152-5000	7b. ADDRESS (City, State and ZIP Code)
8a. NAME OF FUNDING/SPONSORING ORGANIZATION Space and Naval Warfare Systems Command 8b. OFFICE SYMBOL (if applicable) SPAWAR	9. PROCUREMENT INSTRUMENT IDENTIFICATION NUMBER
8c. ADDRESS (City, State and ZIP Code) Washington, DC 20363-5100	10. SOURCE OF FUNDING NUMBERS PROGRAM ELEMENT NO.: RDDA PROJECT NO.: MP57 TASK NO.: AGENCY ACCESSION NO.: DN288 591

11. TITLE (include Security Classification)

Surface-Wave Model Uncertainty Assessment

12. PERSONAL AUTHOR(S)

T.N. Roy, D.B. Sailors, and W.K. Moision

13a. TYPE OF REPORT	13b. TIME COVERED	14. DATE OF REPORT (Year, Month, Day)	15. PAGE COUNT
Final	FROM Oct 1984 TO Sep 1986	November 1987	75

16. SUPPLEMENTARY NOTATION

17. COSATI CODES			18. SUBJECT TERMS (Continue on reverse if necessary and identify by block number)
FIELD	GROUP	SUB-GROUP	ground-wave propagation transmission-loss data surface-wave losses

19. ABSTRACT (Continue on reverse if necessary and identify by block number)

The GROUNDWAVE model is compared to 84 surface-wave measurements made at frequencies of 20, 50, and 101.5 MHz for mountainous, hilly, and flat terrain. Surface wave transmission loss error is evaluated as a function of distance, frequency, terrain and receiving antenna height. The overall average measured transmission loss is 144 dB with an average interdecile range of 11 dB. The overall average calculated transmission loss is 141 dB, well within the interdecile range. When the model was tested as a function of terrain type, a trend toward underestimating the transmission loss as the terrain became more irregular was apparent.

GROUNDWAVE model error is evaluated as a function of input effective ground conductivity and effective ground relative dielectric constant also. By using constant values for these ground constants as a function of frequency, as is the usual practice, the possibility exists for substantial error in transmission loss calculations as a function of frequency. In the frequency range 2 to 20 MHz, results how the GROUNDWAVE model to underestimate transmission loss by an average of 13.1 dB for desert, mountainous, and hilly terrain. For the rich agricultural and marsh terrain, the GROUNDWAVE model overestimated the transmission loss by an average of only 1.9 dB.

When the GROUNDWAVE model predicted transmission losses were compared to measured over-ocean data, it was found that the model severely over-predicted at frequencies greater than 18 MHz. This was attributed to the inability of the model to input nonstandard atmospheres.

20 DISTRIBUTION/AVAILABILITY OF ABSTRACT	21. ABSTRACT SECURITY CLASSIFICATION
☐ UNCLASSIFIED/UNLIMITED ☒ SAME AS RPT ☐ DTIC USERS	UNCLASSIFIED
22a. NAME OF RESPONSIBLE INDIVIDUAL T.N. Roy	22b. TELEPHONE (include Area Code) (619) 553- 3068 22c. OFFICE SYMBOL Code 542

DD FORM 1473, 84 JAN

83 APR EDITION MAY BE USED UNTIL EXHAUSTED
ALL OTHER EDITIONS ARE OBSOLETE

CONTENTS

ILLUSTRATIONS

ILLUSTRATIONS (Continued)

ILLUSTRATIONS (Continued)

TABLES

SUMMARY

OBJECTIVE

Assess the accuracy of the surface-wave model (GROUNDWAVE) and present current computer implementations of the algorithm.

RESULTS

GROUNDWAVE model surface-wave transmission loss calculation error was evaluated as a function of distance, frequency, terrain, and receiving antenna height. The overall average measured transmission loss was 144 dB with an average interdecile range of ± 11 dB. The overall average calculated transmission loss was 141 dB, well within the interdecile range. For the Colorado plains data, the GROUNDWAVE model overestimated the transmission loss by an average of 3.2 dB. The GROUNDWAVE model underestimated the Colorado mountains data transmission loss by an average of 12.9 dB. For the Ohio hills data, the model again overestimated the transmission loss by an average of 2.4 dB.

When the GROUNDWAVE model error was examined as a function of distance, frequency, and receiving antenna height, no clear trend was seen. However, when GROUNDWAVE model error was examined as a function of terrain type, a trend towards underestimating the transmission loss as the terrain became more irregular was apparent.

GROUNDWAVE model error was also evaluated as a function of input effective ground conductivity and effective ground relative dielectric constant. By using constant values for ground conductivity and dielectric constants in the GROUNDWAVE model as a function of frequency, as is the usual practice, the possibility exists for substantial error in transmission-loss calculations as a function of frequency. Results show, in the frequency range 2 to 20 MHz, the GROUNDWAVE model to underestimate the transmission loss by an average of 13.1 dB for desert, mountainous, and hilly terrain. For rich agricultural and marsh terrain, the GROUNDWAVE model overestimated the transmission loss by an average of 1.9 dB.

When the GROUNDWAVE model over-ocean transmission losses were compared to measured data, it was found for the case studied that the transmission loss was severely overestimated for frequencies greater than 18 MHz. This error is due to the inability of GROUNDWAVE to allow for the input of a nonstandard atmosphere.

RECOMMENDATIONS

As a result of this study, the following recommendations are made:

1. that the frequency dependent curves representing the ground conductivity and effective ground relative dielectric constant be incorporated into the GROUNDWAVE model;

2. that the accuracy of the modified version of the GROUNDWAVE model be assessed for the three different types of terrain used here;

3. that GROUNDWAVE be modified to allow the input of a nonstandard atmosphere;

4. that as a separate comparison, determine the accuracy of the GROUNDWAVE model in the Army PROPHET Evaluation System (APES) where these same curves have been implemented in EPM-73;

5. that the GROUNDWAVE model in APES be considered for use when surface roughness (i.e., no winds) is of no concern, particularly if it should prove to be more accurate.

1.0 INTRODUCTION

Tactical communications at HF and low VHF frequencies frequently require short-range, low-power radio systems that rely on ground-wave propagation. Ground-wave propagation is dependent on frequency, path length, and characteristics of both the earth's surface, the atmosphere above it, and transmitter/receiver antenna heights. The ability to predict how variations of these parameters affect surface-wave propagation allows communicators to optimize frequency, antennas, and other circuit parameters for short-range communications systems.

This report will describe results of an uncertainty assessment of GROUNDWAVE, a microcomputer program used at NOSC to calculate the surface-wave transmission loss. The transmission loss is evaluated as a function of distance, frequency, terrain, antenna height, polarization, and sea state. The frequency range of calculation allowed is from 1 to 1000 MHz; however, the program is rarely used above 60 MHz. The program assumes standard atmospheric conditions (four-thirds earth). The characteristics of the earth's surface are assumed to be independent of frequency. The FORTRAN implementation of GROUNDWAVE called GWAVE, is listed in appendix A. The BASIC version of the EPM-73 model algorithm, another ground-wave model used at the Naval Ocean Systems Center (NOSC) on microcomputers, is listed in appendix B.

The GROUNDWAVE model was compared to 84 surface-wave measurements made at frequencies of 20, 50, and 101.5 MHz for three different types of land terrain (Langley and Reasoner, 1970). Surface-wave transmission loss error was evaluated as a function of distance, frequency, terrain, and receiving antenna height. The overall average measured transmission loss was 144 dB with an average interdecile range of ±11 dB. The overall average calculated transmission loss was 141 dB, well within the average interdecile range.

GROUNDWAVE model error was also evaluated as a function of input effective ground conductivity and effective ground relative dielectric constant. By using constant values for ground conductivity and dielectric constant in the GROUNDWAVE model as a function of frequency, the possibility exists for substantial error in transmission-loss calculations as a function of frequency. In the frequency range 2 to 20 MHz, results show the GROUNDWAVE model to underestimate the transmission loss by an average of 13.1 dB for desert, mountainous, and hilly terrain. For rich agricultural and marsh terrain, the GROUNDWAVE model overestimated the transmission loss by an average of 1.9 dB.

GROUNDWAVE was compared for a over-ocean path measured by Hansen (1977) in June 1974. It was found for the case studied that the transmission loss was severely over estimated for frequencies greater than 18 MHz. This error is due to the likelihood that GROUNDWAVE does not allow the input of a nonstandard atmosphere.

2.0 BACKGROUND

Interest in ground-wave propagation began with Sommerfeld's (1909) analysis. Widespread use of these results came with Norton's papers (Norton, 1936; Norton, 1937a; and Norton, 1937b), which reduced Sommerfeld's complex expressions to graphs suitable for engineering applications and extended the results for application to spherical surfaces (Norton, 1941). Since then, no less than 500 papers have appeared on this subject over the past 70 years (for a more complete history, the reader is referred to a thorough summary by Wait (1964) and to a discussion and bibliography by Barrick (1970)).

Nearly all treatments on the subject of ground-wave field strength calculations take the earth surface as a perfectly smooth (planar or spherical) interface between the air and ground or air and water. Barrick (1970, 1971a, and 1971b) developed a method of analyzing radiation and propagation above a surface employing an effective surface impedance to describe the effect of the boundary. The resulting effective surface impedance consists of two terms, the impedance of the lower medium when the surface is perfectly smooth and a term accounting for roughness. The latter term can be complex in general and depends on the strengths of the roughness spectral components present. Using values of surface impedance calculated for the Phillips height spectrum of the ocean wind-wave spatial spectrum, Barrick (1970, 1971a, and 1971b) determined the difference between the basic transmission loss above rough sea and the value above a smooth sea for standard atmospheric conditions.

The classical method of accounting for atmospheric refraction of ground waves is to assume an effective earth radius which is k times the actual earth's radius. This technique is valid where the refractivity versus height profile is approximately linear because the change in ray altitude with ground range turns out to be very close to what one would get if the ray did not curve at all but rather the earth curved a little less. In order to determine k, it is necessary to specify a model atmosphere. Of those models available,the most commonly one used in ground-wave propagation codes is the so called four-thirds earth model which represents a typical value for the central U.S. during the winter season (this model is also commonly called the standard atmospheric model). One computer program called GWSNR (Ground-Wave Signal-to-Noise Ratio) due to Berry (1978) allows the input of any value of k; the determination of k is left to the user.

In 1977, Hansen (1977) reported the results of experimental measurements of basic transmission measurements made between 4 and 32 MHz on a 235-km over-ocean southern California path. His purpose was to verify theoretical calculations of basic ground-wave transmission loss, including the effect of varying sea state as postulated by Barrick. Stepped frequency soundings were taken twice per day for a 1-month period, and hourly for one 24-hour period. In general, the data compared well with theory. The variations in signal during the 24-hour test at frequencies below 20 MHz were consistent with sea state change and somewhat with the recorded winds. However, at frequencies above 20 MHz, the variations in signal strength were quite different and at 32 MHz gave signals at times 25 dB greater than predicted by smooth-earth theory for four-thirds earth model of the atmosphere. He attributed this phenomenon to ducting. Pappert and Goodhart (1979), using calculations involving standard waveguide theory along with available radiosonde data, showed convincingly that this signal enhancement observed on frequencies greater than 20 MHz, relative to that expected on the basis of ground-wave theory for four-thirds earth model of the

atmosphere was due to superrefractive environments. Disparity between the calculated and observed standard deviation was attributed to the likelihood of lateral inhomogeneity of the guide at anytime. It was also shown that an exceptionally strong inversion layer was not required to produce significant enhanced signals.

In an attempt to determine how transmission loss predicted from a ground-wave program is affected by realistic environments and sea state, the ground-wave program GWSNR2 (GWSNR with Barrick's (1971b) sea-state surface impedance added) was run for the same environments and path studied by Pappert and Goodhart (1979). The results are summarized here with additional detail given in appendix C. The average and standard deviation of the refractivity gradient at 1 km for the nine profiles was used to find the average, upper, and lower one-sigma effective earth radii. These radii were then used to calculate the transmission loss for the 235-km southern California path used by Hansen (1977) for his measurements. Calculations were made for sea states 0, 1, and 2. There was a vast improvement over the four-thirds earth model above 20 MHz as was noted by Pappert and Goodhart (1979). The variance of the calculated results increased with increasing frequency in a manner similar to figure 12 of Pappert and Goodhart. For sea state 2 the results were in closer agreement with Hansen's (1977) measured results in the frequency range 4 to 20 MHz than for zero sea state, but the results above 20 MHz were further away than the zero sea state results.

The calculation of transmission loss for ground-wave propagation requires the ground constants conductivity σ and relative dielectric constant ϵ_r. In the past, nominal values for these parameters have been taken from various sources that were for the 550-kHz to 1500-kHz frequency band over large regional areas. Both σ and ϵ_r vary as a function of frequency, water content, geological constituents, temperature, weather, and local anomalies. Hagn, Sifford, and Shepard (1982) have measured these parameters for various types of soils and frequencies, and Wong, Rossiter, Olhoeft, and Strongway (1977) have measured these parameters for permafrost. Exponential curves were fitted to results of these measurements by Sailors, Moision, and Roy (1983).

3.0 SURFACE-WAVE MODEL (GROUNDWAVE)

Tactical communication systems customarily are short-range, low-powered, radio frequency systems that rely on surface-wave propagation. Because surface-wave propagation is highly dependent upon the characteristics of the earth's surface and the transmitter/receiver geometry, the usefulness of a specific power and frequency may be very difficult to assess.

Many models relating required signal power to ground range, frequency, and specific terrain have been developed. For example, Booker and Lugananni (1978) have a model for the propagation loss of vertically polarized signals over a smooth sea at frequencies from 2 to 30 MHz, and for antenna height less than approximately 10 m. Levine (Megatek, 1977) has a similar model, accurate from about 1 to 100 MHz. A more complex model from ECAC (1975) provides propagation losses for any smooth surface (sea, land, and swamp) for low-to-medium antenna heights and for frequencies between 1 and 30 MHz. Lustgarten and Madison (1977) have developed a model that provides the propagation losses for several terrain types, frequencies from 1 to 1000 MHz, and antenna heights up to 3 km. Additionally, Levine (Megatek, 1978) has provided a method for modeling irregular surfaces (rolling hills, etc.) and varying vegetation coverage.

In this section four surface-wave-loss models are examined and three additional models that allow for the effects of rough terrain, ocean waves, and/or surface vegetation are discussed. Sections 4 to 6 will cover in detail a comparison of the various surface-wave-loss models and will discuss the value of alternative formulations.

3.1 THE BOOKER/LUGANANNI MODEL

The Booker and Lugananni model, as well as the Levine model, is based on the work of Barrick (1970, 1971, and 1971b) and is a strictly empirical fit that reduces his expressions into a tractable form.

Following Barrick (1970, 1971a, and 1971b), this model considers the surface-wave losses for antennas located at the sea surface, using vertically polarized signals.

The surface-wave loss can be broken into two components: (1) that due to loss as the signal travels a distance R across a smooth, flat, perfectly conducting surface, and (2) corrections for the earth's curvature and a lossy surface. The first term is related to free space losses, while the second term is an approximation to figure 8 of Barrick (1970, 1971a, and 1971b), shown here as figure 1.

The surface-wave loss expression provided by Booker and Lugananni (1978) is

$$Lg = 20 \log_{10} \frac{2\pi Rf}{0.3} + C_1(f)\, R^{C_2(f)} \quad \text{(in dB)}, \tag{1}$$

where R is the distance between transmitter and receiver in km, f is the frequency in MHz, and

$$C_1(f) = (1.78 \times 10^{-4})\, f^{2.55} \exp -(1.40 \times 10^{-8})\, f^{5}\,, \tag{2}$$

$$C_2(f) = 1.83\, f^{-0.243}\,. \tag{3}$$

The fit achieved by Booker and Lugananni to Barrick's curves is extremely accurate in the frequency regime from 2 through 30 MHz (within 2 dB), but degrades very rapidly outside that window.

3.2 THE LEVINE MODEL

This model, as with the Booker/Lugananni model, is an empirical fit to Barrick's low-antenna height, smooth-ocean-surface propagation. Although the accuracy of the fit is not as good as the Booker/Lugananni model in the 2- to 30-MHz band, it does fit the Barrick curves reasonably well (±4 dB) up to almost 100 MHz, and can prove a useful addition.

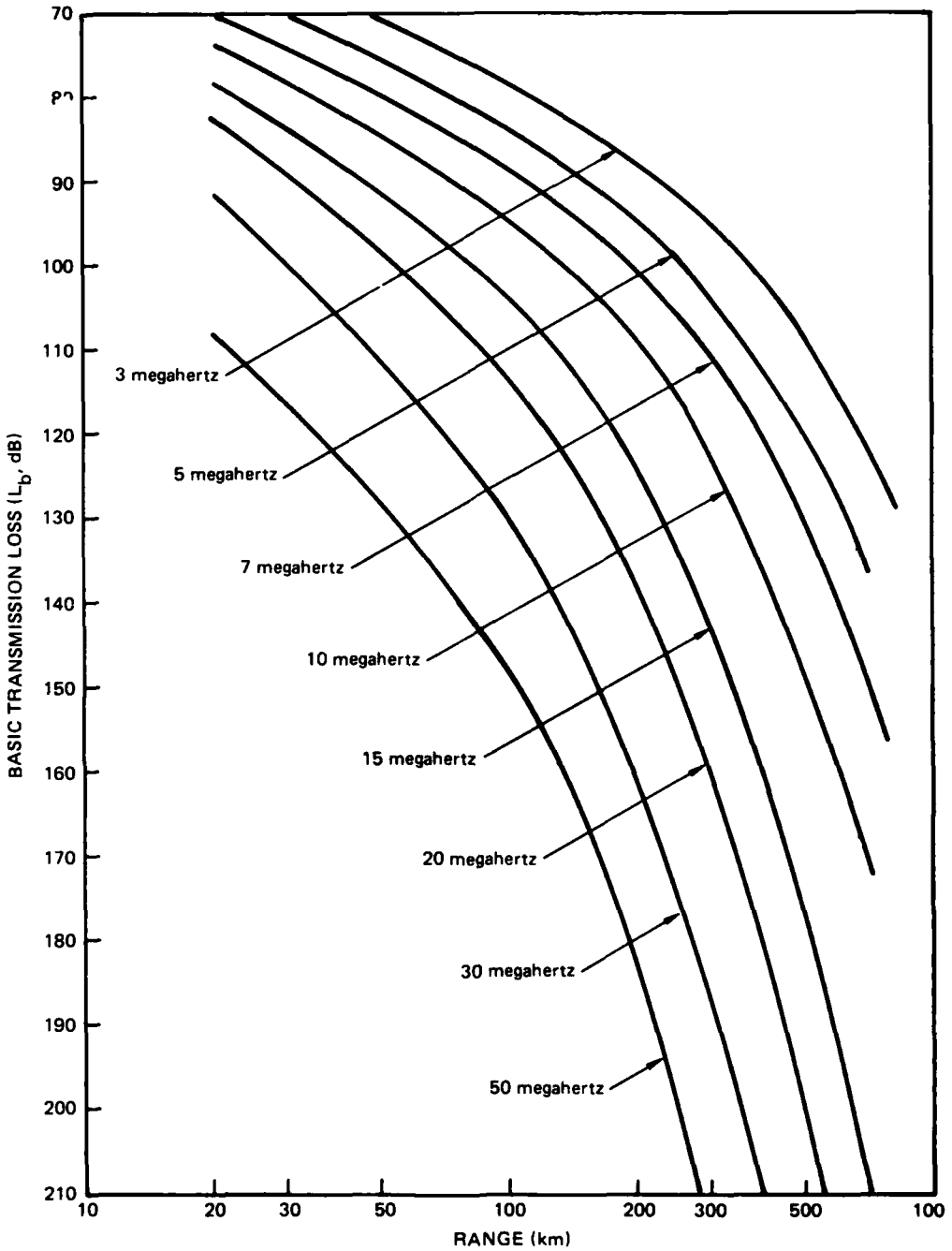

Figure 1. Basic transmission loss across the ocean between points at the surface of smooth spherical earth. Conductivity is 4 mhos/m and an effective radius of 4/3 is assumed.

The loss is written in two terms, as in the Booker/Lugananni model, with a free space loss related term, and an approximation accounting for the additional losses due to curvature and finite earth conductivity:

$$Lg = 20 \log_{10} \frac{2\pi Rf}{0.3} + 1.45 \exp [-f/500 \quad f \quad (R/140)]^{exp}$$

$$(-0.008 \ (f^{3})). \tag{4}$$

3.3 THE ECAC MODEL

The ECAC model was designed to compute the surface-wave transmission loss over a smooth, spherical earth for vertically or horizontally polarized signals between 1 and 30 MHz. This model uses a theoretical formulation that differentiates between distances short enough to assume planar earth, and longer distances where the earth's curvature becomes important.

The separation distance between the planar and curved earth models was empirically found to be

$$d_c = 150/f^{.5305} \qquad [d_c \text{ in km, f in MHz}]. \tag{5}$$

In the planar region, the ECAC model may be summarized:

$$Lg = L_{FS} - 6 \qquad [d < 1/2 \ d_{FSM}], \tag{6}$$

$$Lg = L_{FS} + 120 \log_{10} d/d_{FSM} \qquad [d_{FSM}/2 \leq d \leq d_c], \tag{7}$$

where

$$L_{FS} = \text{free space loss} \tag{8}$$

and

$$d_{FSM} = \frac{h'_1 h'_2}{79.6\lambda}$$

with

d = separation distance (km)

λ = wavelength (m)

h'_1, h'_2 are the effective antenna heights.

Effective antenna heights can be calculated using

$$h'_1, h'_2 = \sqrt{h_1^2 + h_0^2}, \ \sqrt{h_2^2 + h_0^2} \tag{9}$$

where

h_1, h_2 are antenna feed heights

h_0 = minimum effective height

with

$$h_0 = \frac{\lambda[\epsilon_r^2 + (0.06\lambda\sigma)^2]^{1/2}}{2\pi\,[(\epsilon_r - 1)^2 + (0.06\lambda\sigma)^2]^{1/4}} \quad \text{for vertical polarization,} \tag{10}$$

and

$$h_0 = \frac{\lambda}{2\pi\,[(\epsilon_r - 1)^2 + (0.06\lambda\sigma)^2]^{1/4}} \quad \text{for horizontal polarization,} \tag{11}$$

with ϵ_r = dielectric constant

σ = conductivity (mmhos/m).

When antenna separations exceed d_c, then the earth's curvature begins to play a role. The ECAC model fits this added loss as increasing linearly with distance. The major part of this calculation is to determine the slope of this increase.

For vertical polarization, intermediate parameters defined as follows are calculated:

$$X = 60\,\lambda\sigma$$

$$b' = \tan^{-1}\,[(\epsilon - 1)/X]$$

$$b'' = \tan^{-1}\,(\epsilon/X)$$

$$K = 0.031\,\lambda^{1/3}\,(X \cos b'/\cos^2 b'')^{1/2}$$

$$b = 2b'' - b'$$

$$\beta_0(K) = 1.607 - K \sin\left(\frac{3\pi}{4} - \frac{b}{2}\right) - 1.237\,K^3 \sin\left(\frac{7\pi}{12} - \frac{5b}{2}\right)$$

$$+ 0.4\,K^4 \sin(\pi - 2b) - 2.755\,K^5 \sin\left(\frac{5\pi}{12} - \frac{5b}{2}\right); \quad (k \leq 0.5) \tag{12}$$

$$\beta_0 = 0.7003 - \frac{0.61834}{K} \sin\left(\frac{b}{2} - \frac{13\pi}{12}\right) - \frac{0.23642}{K^2} \sin\left(b - \frac{\pi}{2}\right)$$

$$+ \frac{0.05339}{K^3} \sin\left(\frac{3b}{2} - \frac{11\pi}{12}\right) - \frac{0.002255}{K^4} \sin\left(2b - \frac{4\pi}{3}\right); \quad (K \geq 0.8) \tag{13}$$

If $0.5 \leq K \leq 0.8$, equation 12 is solved for $K = 0.5$ and equation 13 is solved for $K = 0.8$. The results are then averaged.

For horizontal polarization $\beta_0 = 1.607$.

Finally, the surface-wave path-loss slope, M, may be calculated using

$$M = 0.0572\ \beta_0\ f_{MHz}^{1/3} - 0.1 \quad \text{(dB/km)}. \tag{14}$$

The surface-wave loss is then calculated using

$$Lg = L_{FS} + 20\ \log_{10}\ d_c/d_{FSM} + M\ d\text{-}d_c \qquad d \geq d_c\ . \tag{15}$$

Note that although this is much more flexible and versatile than the previous two models, a price is paid in the complexity.

3.4 THE LUSTGARTEN/MADISON MODEL

The Lustgarten/Madison empirical propagation model, henceforth called EPM-73, is similar to the ECAC model in including direct ray, reflected ray, and the surface wave, but also includes troposcatter effects at greater distances. This model has two sections, determined by the ratio of the antenna height (h) to the wavelength (λ), hence the terminology high-h/λ and low-h/λ. The low-h/λ model is similar to Bullington (1947), while the high-h/λ model is a simple version of smooth-earth theory. There is a transition region, which is dealt with by using both models and picking the larger loss as the best estimate of the loss.

The high-h/λ model is portrayed graphically in figure 2. There are three regions of interest: the reflection region, the diffraction region, and the troposcatter region. The distance d_{FSRF} is the distance where diffraction becomes significant, the model uses d_1, which is scaled at 1.1 d_{FSRF}. The distance d_2 is that at which troposcatter effects begin to dominate. In this formulation, d is in kilometers (km), the antenna height (h_1,h_2) and wavelength (λ) are in meters (m) and the frequency (f) is in megahertz. The radio-line-of-sight distance is defined as

$$d_{LOS} = \sqrt{17}\ h_1 + \sqrt{17}\ h_2. \tag{16}$$

Empirical formulas for d_1 are as follows:

$$d_1 = \frac{1.1\ h_1 h_2 f}{3.47\ x\ 10^5} \qquad h_1 h_2 f \leq A\ , \tag{17}$$

$$d_1 = 1.1\ p\ d_{LOS} \qquad h_1 h_2 f \leq A\ , \tag{18}$$

where

$$A = \frac{2.08\ x\ 10^6\ d_{LOS}}{10^3 - 3.75\ d_{LOS}} \tag{19}$$

and

$$p = 0.6 \times 1.08 \times 10^{-8} h_1 h_2 f \qquad (p \leq 0.9) \qquad (20)$$

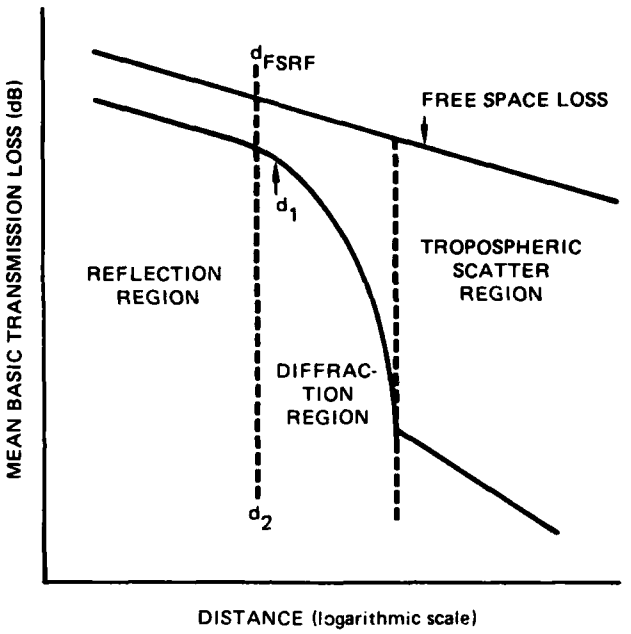

Figure 2. High-h/λ model from Lustgarten and Madison, (1977).

The empirical formulas for d_2 are

$$d_2 = d_{LOS} - 48.3 \log_{10} f + 163 \qquad (40 \leq f < 160 \text{ MHz}), \qquad (21)$$

$$d_2 = d_{LOS} - 16.1 \log_{10} f + 91.8 \qquad (f > 160 \text{ MHz}), \qquad (22)$$

and for vertical polarization over seawater

$$d_2 = -4 d_{LOS} - 1.29 f + 406 \qquad (f < 255 \text{ MHz}). \qquad (23)$$

The surface-wave loss terms become, in terms of these distances

$$Lg = L_{FS} + 5 \qquad (d \leq d_1) \qquad (24)$$

$$Lg = L_{FS} + 5 + 50(d - d_1)/(d_2 - d_1) \qquad (d_1 < d \leq d_2), \qquad (25)$$

$$Lg = L_{FS} + 55 + x \log d/d_2, \qquad (26)$$

where

$$x = 20 \qquad (1 \leq d/d_2 \leq 4)$$

$$x = 5d/d_2 \qquad (4 < d/d_2 < 8)$$

$$x = 40 \qquad (d/d_2 \geq 8)$$

and

L_{FS} is the free space loss,

$$L_{FS} = 33 + 20 \log_{10}(f) + 20 \log_{10}(d). \quad (27)$$

The low-h/λ model is portrayed graphically in figure 3, and, as in the high-h/λ model, has three main regions of interest (with boundary distances). The cosite region is not included in this model, where d_{CF} defines the upper limit to the cosite region. The distance d_c (as in the ECAC model) defines the boundary for the plane and curved earth models. The effective height h' is achieved exactly as in the ECAC model, although h_0 is assumed to be zero for all horizontally polarized propagation.

The formulas for the boundary-distances are

$$\log_{10} d_{CF} = \log_{10} f + 0.75 \log_{10} h'_1 h'_2 - 3.92, \quad (28)$$

$$d_c = 129/f^{1.2} \qquad (f \leq 100 \text{ MHz}), \quad (29)$$

$$d_c = 59.9/f^{1/3} \qquad (f > 100 \text{ MHz}), \quad (30)$$

and d_2 is as defined for the high-h/λ model.

The low-h/λ model is only applicable when $d_{CF} \leq d_c$ and $d \geq d_{CF}$. The loss formulas are then

$$Lg = 111 - 15 \log_{10} h'_1 h'_2 + 40 \log_{10}(d) \qquad (d_{CF} \leq d \leq d_c), \quad (31)$$

$$Lg = 111 - 15 \log_{10} h'_1 h'_2 + 40 \log_{10}(d_c) + 20 \log_{10} d/d_c + 0.62 M \, d - d_c \qquad (d_c < d \leq d_2), \quad (32)$$

$$Lg = 111 - 15 \log_{10} h'_1 h'_2 + 40 \log_{10}(d_c) + 20 \log_{10} d_2/d_c + 0.62 M \, d_2 - d_c + 40 \log_{10} d/d_2 \qquad (d > d_2), \quad (33)$$

where

$M = f^{1/2}/20$ for vertical polarization over seawater in the frequency range $1 \leq f \leq 10$ MHz,

$M = 0.5 \log_{10}(f) - 0.35$ for vertical polarization over seawater for the frequency range $10 < f \leq 100$ MHz,

$M = 0.25 \log_{10}(f) + 0.06$ for vertical polarization over marsh land for the frequency range $1 \leq f \leq 10$ MHz,

and

$M = f^{1/3}/7$ for all other polarization and land-condition combinations. The maximum allowed value of M is 0.5 for all conditions.

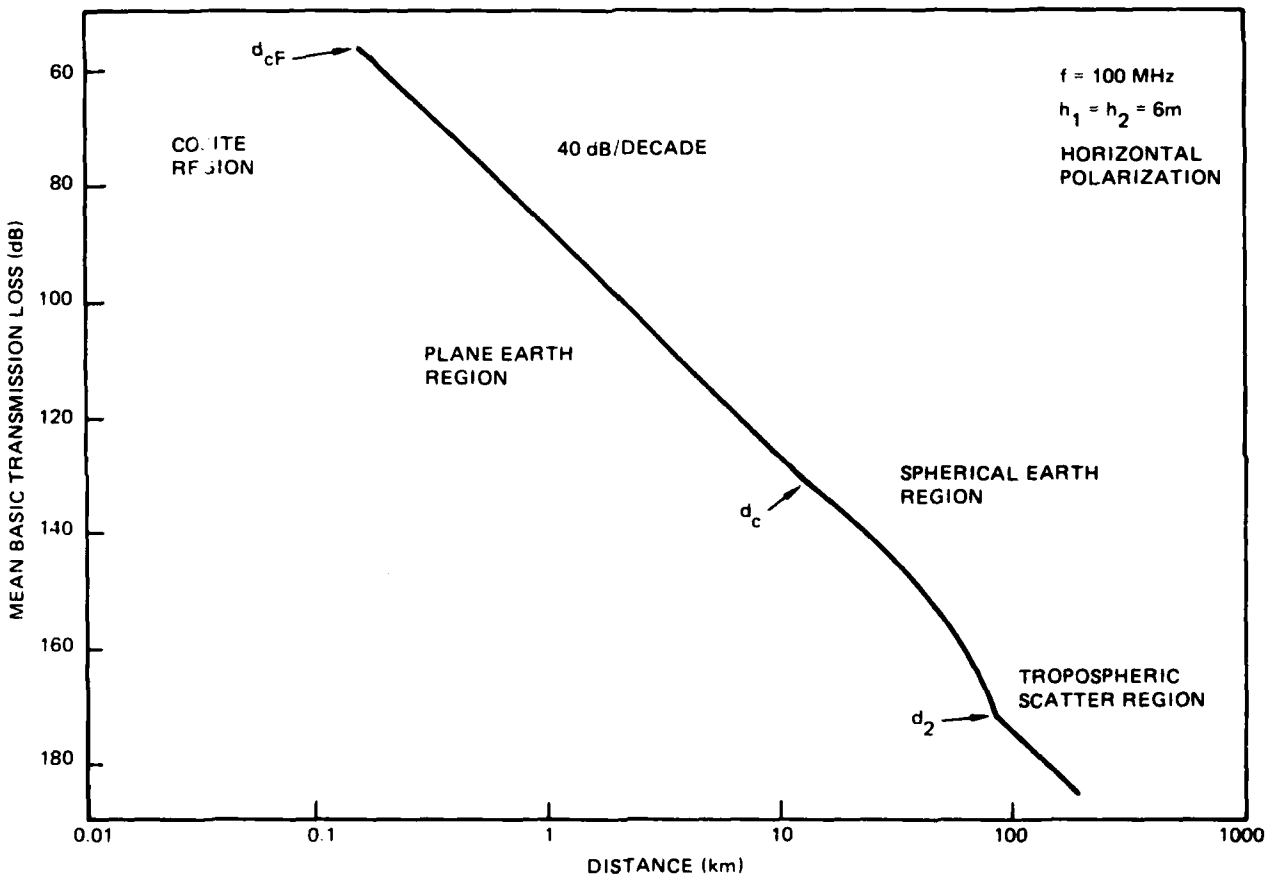

Figure 3. Sample prediction of the low h/λ EMP-73 model from Lustgarten and Madison, 1977.

3.5 LEVINE'S ROUGH-TERRAIN AND SURFACE-VEGETATION MODELS

Levine followed Barrick by incorporating surface roughness effects through the surface impedance. Given a smooth surface impedance Δ_c, Levine calculates the modified surface impedance for a wavy surface with a single wave number $r = 2\pi/L$ (with L the horizontal spacing between peaks) and rms wave height, S (or alternatively rms surface roughness),

$$\Delta_{eff} = \Delta_c + \frac{S^2 r^2}{2} \left[\Delta_c + \frac{k}{2r}^{1/2} (1 + i)\right] . \tag{34}$$

The surface impedance, for a spherical earth with conductivity σ and dielectric constant ϵ, is given by

$$\Delta = \frac{ik}{\gamma} \sqrt{1 + k^2/\gamma^2} , \tag{35}$$

where $k = 2\pi/\lambda$, with λ the free space wavelength, and (36)

$$\gamma = i\sigma\mu\omega - \epsilon\mu\omega^2 . \tag{37}$$

In general, to include a surface layer with surface impedance $\Delta\ell$ and thickness ℓ, the composite impedance Δ_c is given by

$$\Delta_c = \Delta\ell \frac{\left(\frac{\gamma_\ell}{\gamma_s}\right)^2 \left[\frac{\gamma_s^2 + k^2}{\gamma_\ell^2 + k^2}\right]^{1/2} + \tanh\left[\ell\left(\gamma_\ell^2 + k^2\right)^{1/2}\right]}{1 + \left(\frac{\gamma_\ell}{\gamma_s}\right)^2 \left[\frac{\gamma_s^2 + k^2}{\gamma_\ell + k}\right]^{1/2} \tanh\left[\ell\left(\gamma_\ell^2 + k^2\right)^{1/2}\right]} \tag{38}$$

As in the ECAC model, the EPM-73 formulation for surface impedance is not used directly, and we need to invert the Δ formulation to provide σ, ϵ values. This formulation proceeds as follows

$$\Delta\ \gamma^2 - ik\gamma - ik^2 = 0 \tag{39}$$

or

$$\gamma = \frac{ik \pm \sqrt{-k^2 + 4i\Delta k^2}}{2\Delta} = k\ \frac{i \pm \sqrt{-1 + 4i\Delta}}{2\Delta} \tag{40}$$

and $\sigma = 1/\omega\ \mathrm{Im}\ \{\gamma^2\}$,

$$\epsilon = -\frac{1}{\omega^2}\ \mathrm{Re}\ \{\gamma^2\}.$$

For sea surfaces Levine uses the Phillips spectrum, and obtains

$$L = 2\pi/r = \pi\, u^2/g, \tag{41}$$

$$S = L/20\pi\ , \tag{42}$$

where g = force of gravity = 10 m/s^2

and u is the wind speed in m/s.

Levine represents the surface vegetation as a layer with conductivity 0.00025 Mhos/m and dielectric constant 1.25 with a thickness determined by the degree of forestation. A dense jungle might be 16 m thick, while normal forests may be closer to 8 m, and thick underbrush 1 or 2 m.

3.6 THE ARGO ROUGH-SEA-SURFACE MODEL

The two Levine models are well suited for use in the ECAC and EPM-73 models, which use the conductivity and dielectric constant to calculate the ground losses. Neither the very simple Booker/Luganannni model, nor the Levine surface-wave loss model incorporate those features, and yet a user may very well wish to include sea roughness. Therefore, an empirical fit to Norton's (1957) model was developed which included additional loss incurred upon propagation across a rough sea.

The model fits empirical data that show the added loss and can be described by

$$\text{loss} = C(f,d)\ (\text{wind velocity})^{n(f)}\ . \tag{43}$$

Tne empirical fit described here is indicated by the open circles. In fact, the curves of figure 4 show that the added loss goes to a minimum value (for a given frequency and wind) at some distance, and does not decrease as the distance decreases. This minimum distance is found to be

$$d_{min} = 157\log_{10}f - 137. \tag{44}$$

The loss factor becomes

$$n = 7.2896f^{\,-0.4477}\ , \tag{45}$$

$$C(f,d) = (d'/1000)^{B}\ 0.00337\ (f-9)^{1.0047} \tag{46}$$

where

$$d' = \max\ (d,\ d_{min}).$$

This model is accurate to within 1 dB for frequencies between 10 and 50 MHz and distances from 10 km to 1000 km. For higher frequencies up to approximately 100 MHz, the accuracy is within approximately 3 dB, while for frequencies below 10 MHz, there may be large errors.

3.7 SURFACE-WAVE PROPAGATION EFFECTS

The surface-wave loss is a function of frequency, path length, ground type, and signal polarization, as well as transmitting and receiving antenna heights. The models described in the previous sections allow the user to examine the effects that varying these parameters will have on the surface-wave signal loss. The following section will describe the types of loss variations found by such a parametric study.

As the receiver moves away from the transmitter, the signal falls off, and so for a given power and receiver sensitivity there is a maximum range for usable communication. Figure 5 shows this typical falloff at several frequencies. For vertical polarization the surface-wave loss also increases. At the higher frequencies (>50 MHz) and longer ranges, there is a sharp change in the slope of the loss curve, representing the phenomenon of troposcatter. Because of this scattering phenomenon the signal can propagate to ranges far beyond that expected due solely to diffraction.

Figure 6 shows the effect of varying the polarization for 30 MHz over a sea water path. Note the horizontally polarized signal is more than 40 dB below the vertical, indicating the loss due to ground currents excited by a horizontal E-field.

Figure 7 shows the effect of terrain type on the propagation signal. Sea water has by far the least amount of loss with the land type terrains falling a full 20 dB below signal.

As the receiving antenna (or transmitting antenna) is raised above the earth, the signal loss decreases. Figure 8 shows that this decrease in loss is a function of frequency, with significant effects as the high frequency antennas are raised above approximately 100 m. The upper endpoint of each curve occurs because the model applicability ends there.

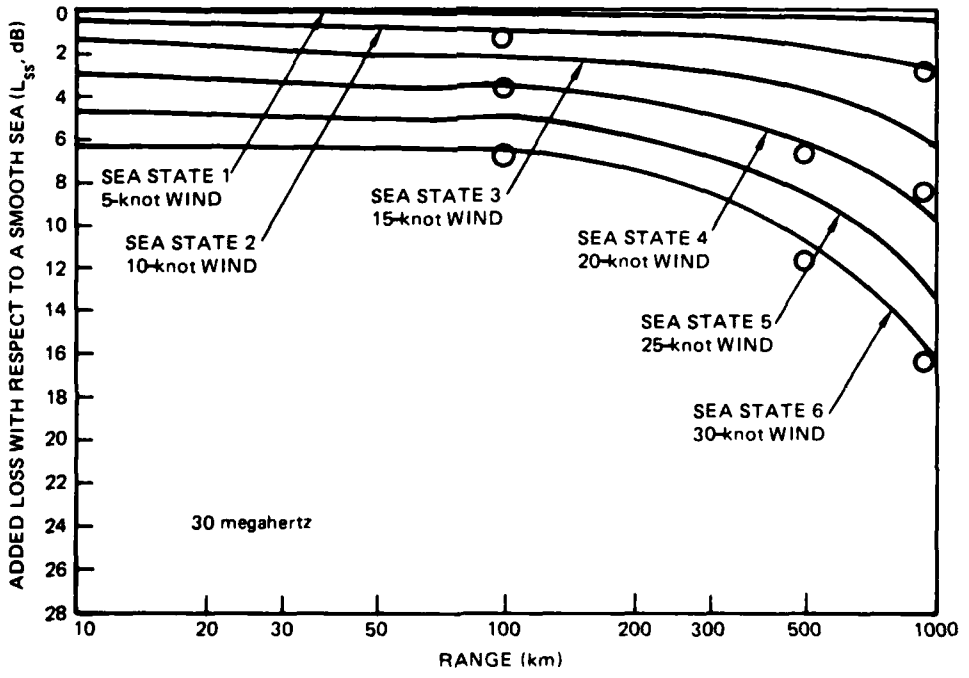

Figure 4. The added loss due to rough sea states, as calculated by Barrick, 1970.

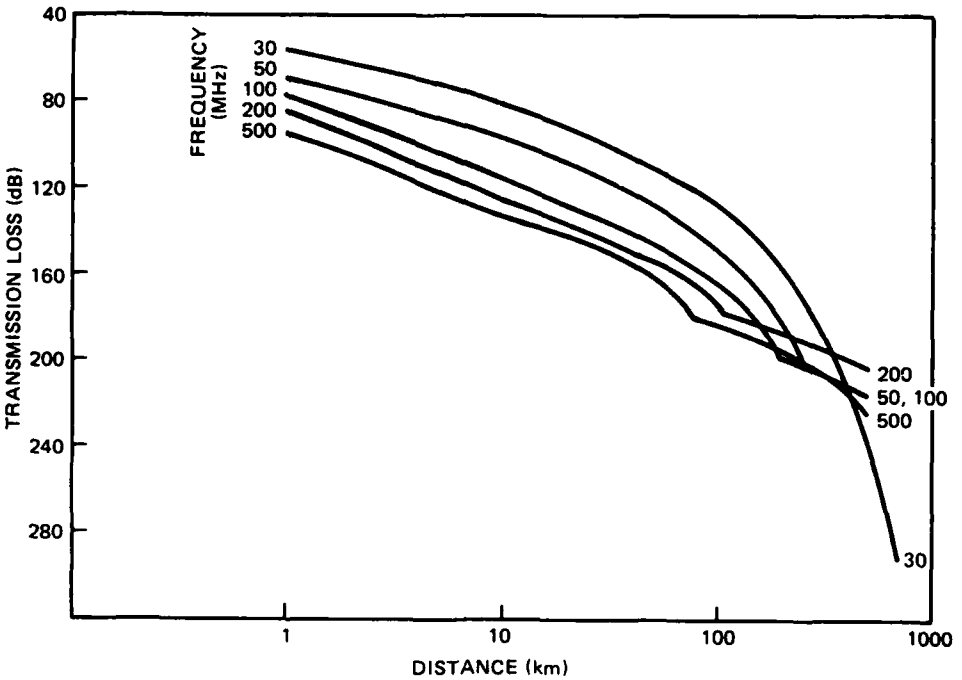

Figure 5. The surface-wave loss for a vertically polarized signal (over sea) at several frequencies, as a function of distance.

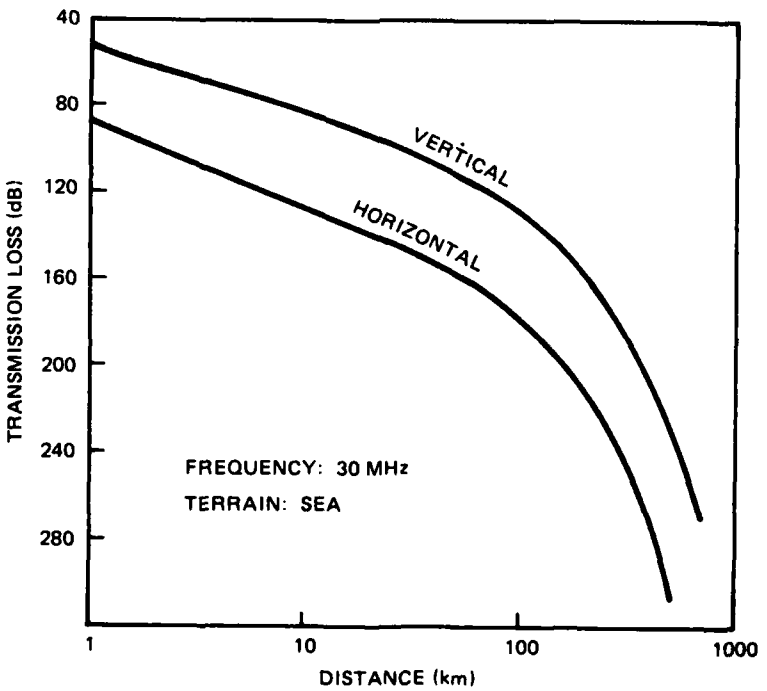

Figure 6. The surface-wave loss for both vertical and horizontal polarization (over sea) showing the increased loss for horizontally polarized signals.

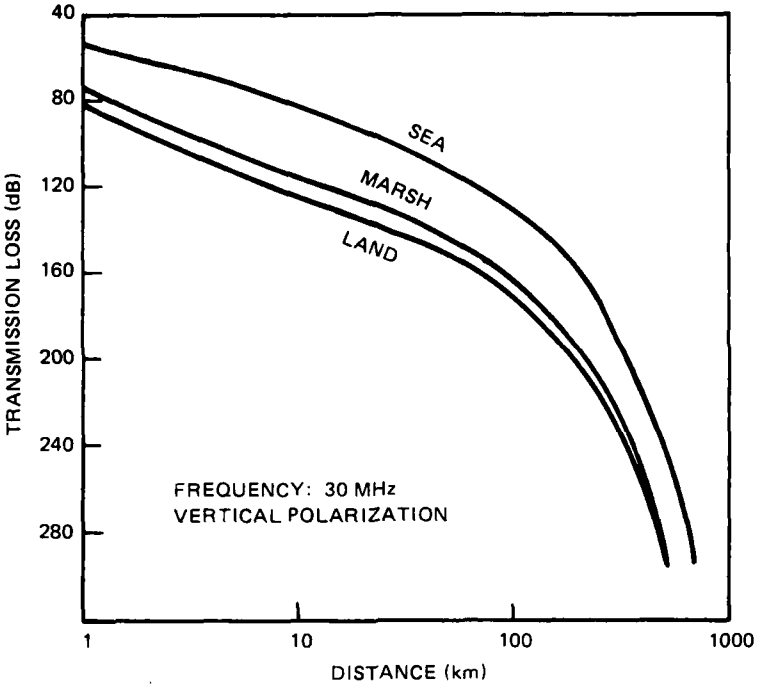

Figure 7. Surface-wave loss for a 30-MHz signal over various terrains.

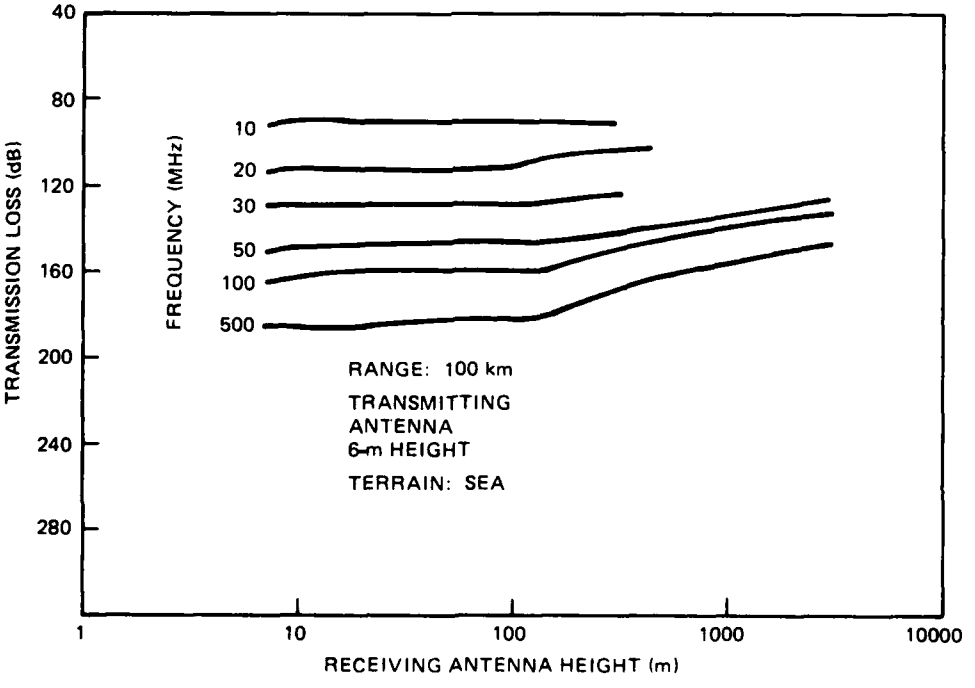

Figure 8. The effect of changing antenna heights on the surface-wave loss.

4.0 DESCRIPTION OF MEASURED LAND TRANSMISSION-LOSS DATA

Basic transmission-loss measurement data required for the GROUNDWAVE model uncertainty assessment over land was taken from Langley and Reasoner (1970). This set of data was chosen because the terrain type and antenna heights were carefully documented over the entire propagation path. A total of 84 surface-wave measurements with median values and interdecile ranges representing hundreds of individual measurements were analyzed. The data included transmission-loss values for frequencies of 20, 50, 101.5, and 101.8 MHz. Terrain types included were Colorado mountains, Colorado plains, and Ohio hills. Several different antenna heights were also used in the measurements. Table 1 lists the surface-wave propagation path data used for the GROUNDWAVE model error analysis.

Table 1. Description of surface-wave propagation path data used for GROUNDWAVE model uncertainty assessment.

Terrain Type	Frequency (MHz)	Distance (km)	Antenna Height (m) Transmit	Receive
Colorado Mountains	20.0	3 to 50	3.3	1.3
	50.0	3 to 50	4.0	0.55
	50.0	3 to 50	4.0	1.7
	101.5	3 to 50	4.0	3.0
	101.5	3 to 50	4.0	6.0
	101.5	3 to 50	4.0	9.0
Colorado Plains	20.0	10 to 50	3.3	1.3
	50.0	10 to 50	4.0	0.55
	50.0	10 to 50	4.0	1.7
	101.5	10 to 50	4.0	3.0
	101.5	10 to 50	4.0	6.0
	101.5	10 to 50	4.0	9.0
Ohio Hills	20.0	10 to 50	3.68	3.0
	50.0	10 to 50	4.24	1.0
	50.0	10 to 50	4.24	3.0
	101.8	10 to 50	4.0	3.0
	101.8	10 to 50	4.0	6.0
	101.8	10 to 50	4.0	9.0

5.0 DISCUSSION OF ACCURACY FOR LAND PATHS

This section will discuss the results of the comparison of median observed transmission-loss data for Colorado plains, Colorado mountains, and Ohio hills to the GROUNDWAVE model. In addition to the error discussion for these three propagation paths, GROUNDWAVE error as a function of distance, frequency, receiver antenna height, terrain type, effective ground conductivity, and effective ground relative dielectric constant will also be discussed.

5.1 COLORADO PLAINS PROPAGATION PATH

Colorado plains measurements were made over about 190 paths at nominal distances of 3, 5, 10, 20, 30, and 50 km from the common transmitter. Transmitter antenna heights ranged from 3.3 to 4.0 m and receiver antenna heights ranged from 0.55 to 9.0 m. Exact frequencies used were 20.08, 49.72, and 101.5 MHz.

For a frequency of 20 MHz, figure 9 shows Colorado plains median transmission loss and the GROUNDWAVE model results plotted as a function of distance. Transmitter antenna height, T_h, was 3.3 m and receiver antenna height, R_h, was 1.3 m. The calculated transmission loss differed from the observed by 4 or 5 dB at short ranges and 3 dB or less at long ranges. The average bias for the range 3 to 50 km was 0 dB.

Figure 10 shows Colorado plains and GROUNDWAVE model results for a frequency of 50 MHz and transmitter and receiver antenna heights of 4.0 and 0.55 m, respectively. The model compared well with the observed data at short range and an average bias for the range 3 to 50 km was -3.5 dB.

Figure 11 shows comparison results for the same set of conditions except that the receiver antenna height has been raised to 1.7 m. Model values are within the interdecile ranges for all distances. The model predicted more transmission loss than was observed. The average bias was -4.5 dB.

In figure 12, the terrain is the same but the frequency has increased to 101.5 MHz and the receiver antenna height is now 3.0 m. Model values are within the interdecile ranges for all distances except 20 km. Average bias was -3.3 dB, indicating the model slightly overestimated the transmission loss.

The receiver antenna height was increased to 6 m and the resulting transmission-loss data for Colorado plains is plotted in figure 13. GROUNDWAVE model values are within the interdecile ranges for all distances. An average bias of -3.5 dB indicates the model overestimates the transmission loss for these conditions.

In figure 14, the model and observed data are compared with the receiving antenna raised to 9 m. Model values are still within the interdecile ranges for all distances. The model overestimates the transmission loss for this set of data. The average bias was -4.3 dB.

The GROUNDWAVE model overestimated the transmission loss for all Colorado plains measurement paths. The overall average bias for all conditions was very small, -3.2 dB. It is interesting to note that in all the tests, except the one represented by figure 9, the overestimation of the transmission loss was always largest at a distance of 20 km.

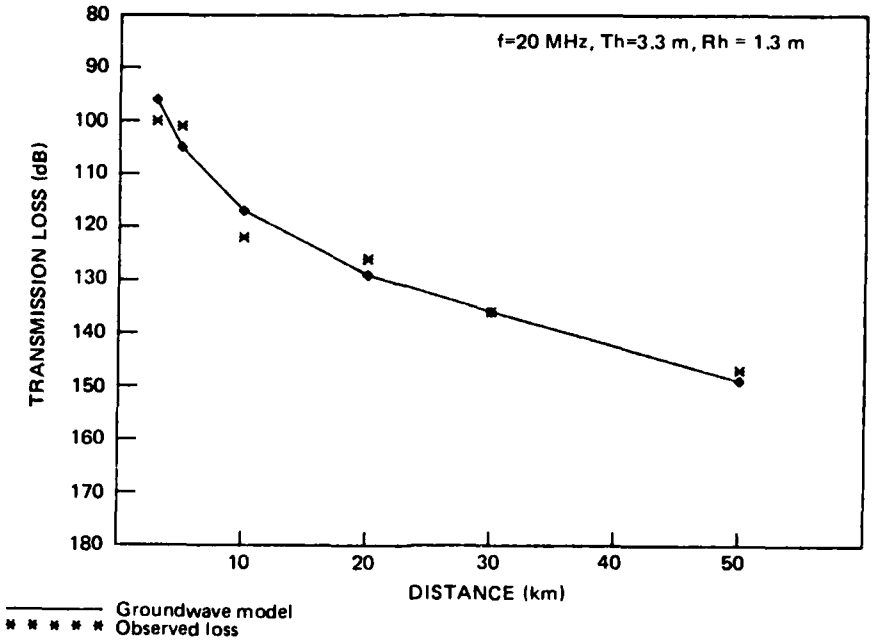

Figure 9. Colorado plains median observed transmission-loss data compared to the GROUNDWAVE model as a function of distance, f=20 MHz, T_h=3.3 m, R_h=1.3 m.

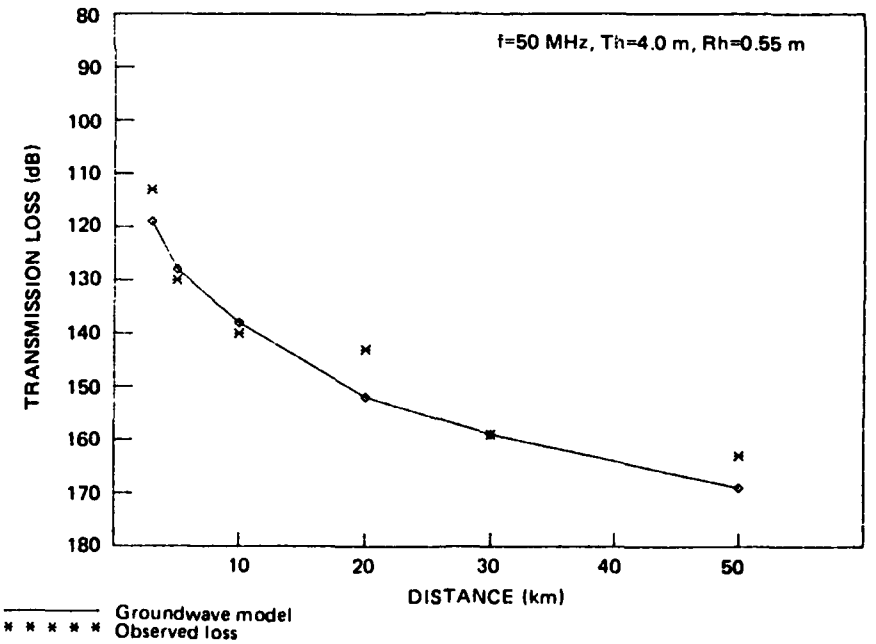

Figure 10. Colorado plains median observed transmission-loss data compared to the GROUNDWAVE model as a function of distance, f=50 MHz, T_h=4.0 m, R_h=0.55 m.

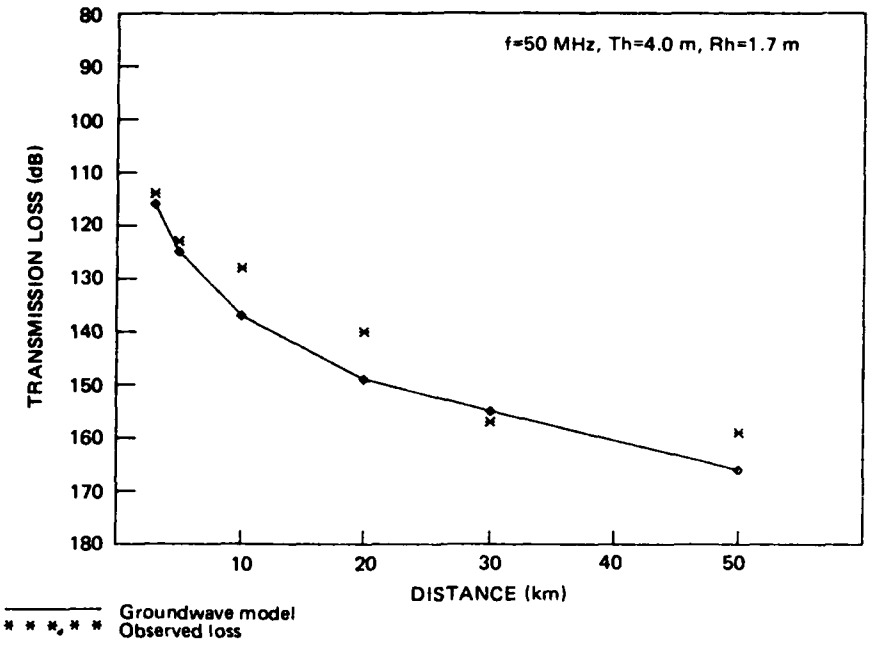

Figure 11. Colorado plains median observed transmission-loss data compared to the GROUNDWAVE model as a function of distance, f=50 MHz, T_h=4.0 m, R_h=1.7 m.

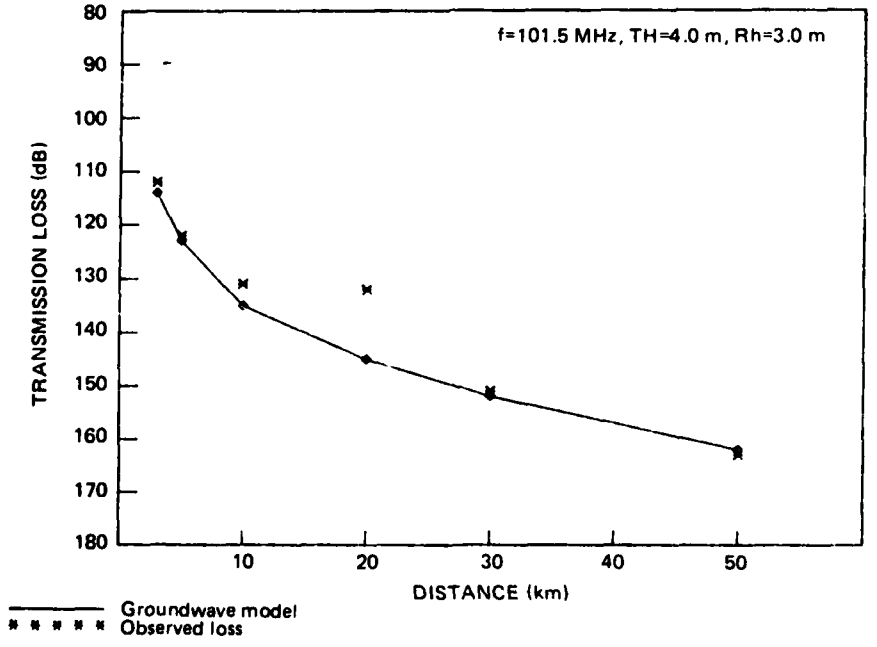

Figure 12. Colorado plains median observed transmission-loss data compared to the GROUNDWAVE model as a function of distance, f=101.5 MHz, T_h=4.0 m, R_h=3.0 m.

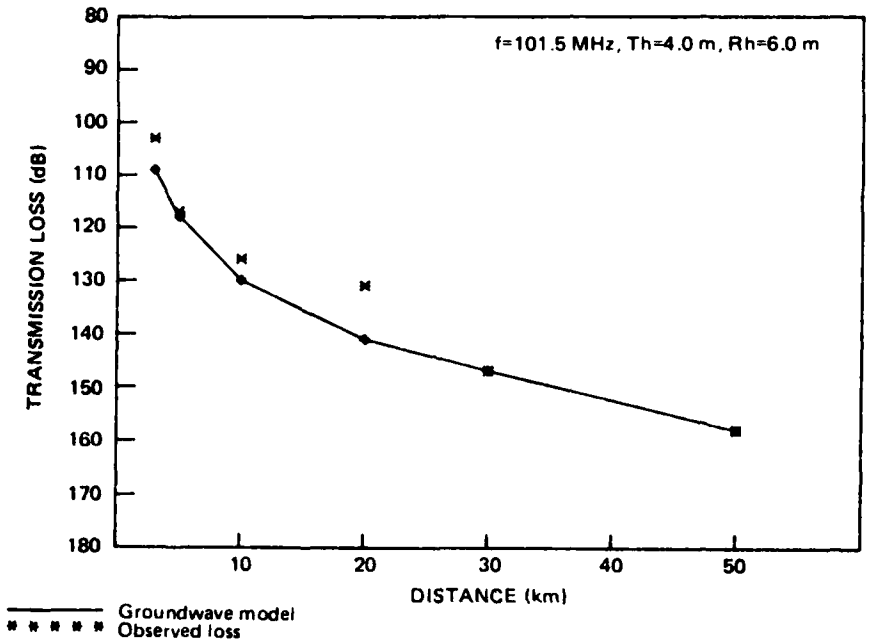

Figure 13. Colorado plains median observed transmission-loss data compared to the GROUNDWAVE model as a function of distance, f=101.5 MHz, T_h=4.0 m, R_h=6.0 m.

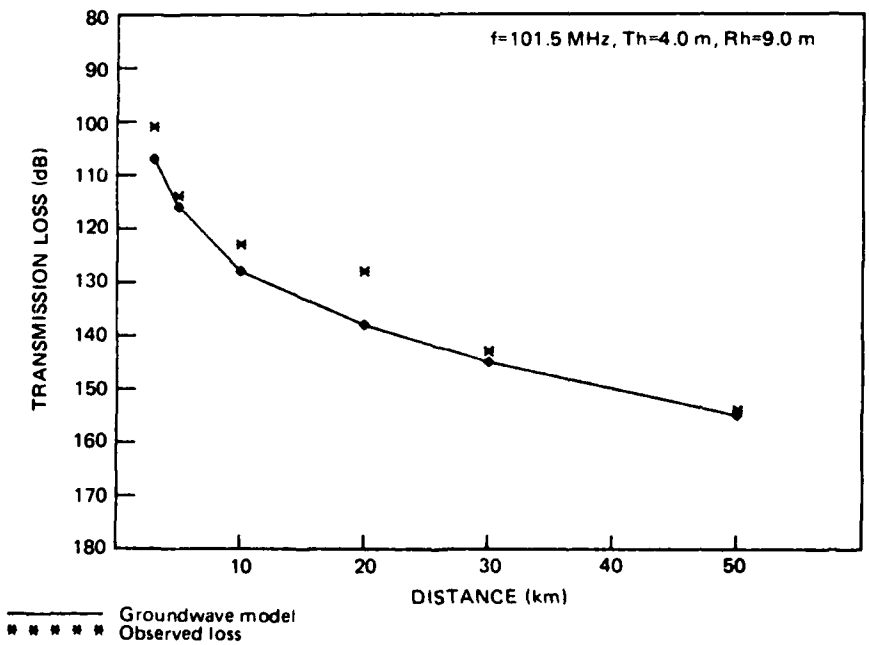

Figure 14. Colorado plains median observed transmission-loss data compared to the GROUNDWAVE model as a function of distance, f=101.5 MHz, T_h=4.0 m, R_h=9.0 m.

5.2 COLORADO MOUNTAINS PROPAGATION PATH

Colorado mountains measurements were made over 46 paths at nominal distances of 10, 20, 30, and 50 km from the transmitter. Transmitter antenna heights ranged from 3.3 to 4.0 m and receiver antenna heights ranged from 0.55 to 9.0 m. Exact frequencies used were 20.08, 49.72, and 101.5 MHz.

In figure 15, the Colorado mountains median transmission-loss data and the GROUNDWAVE model results are plotted as a function of distance for a frequency of 20 MHz. Transmitter antenna height was 3.3 m and the receiver antenna height was 1.3 m. Model values are outside the interdecile ranges except at 50 km. The model underestimates the transmission loss with an average bias of +19.2 dB.

A new set of conditions is shown in figure 16. The frequency has increased to 50 MHz, transmitter antenna was raised to 4.0 m and the receiver antenna was lowered to 0.55 m. Model values are within the interdecile ranges for all distances. The model underestimates the transmission loss with an average bias of +5.7 dB.

Figure 17 shows comparison results for a receiver height of 1.7 m. Model values are within the interdecile ranges for all distances except 20 km. The model still underestimates the transmission loss with an average bias of +6.5 dB.

The frequency was increased to 101.5 MHz and the receiver antenna was raised to 3.0 m for the set of data plotted in figure 18. Model values are outside the interdecile ranges for all but the 10 km distance. Transmission loss is underestimated, having an average bias of +13.0 dB.

The receiver antenna height was raised to 6 m and the resulting transmission-loss data for Colorado mountains is plotted in figure 19. GROUNDWAVE model values are outside the interdecile ranges for all but the 10 km distance. An average bias of +15.7 dB indicates the model underestimates the transmission loss for these conditions.

In figure 20, the model and observed data are compared with the receiving antenna raised to 9 m. Again, model values are outside the interdecile ranges, except at 10 km. Average bias was +17.0 dB indicating a large GROUNDWAVE underestimation of the transmission loss.

The GROUNDWAVE model underestimated the transmission loss for all Colorado mountains measurement paths. The overall bias for all paths was large, +12.9 dB. At 20 MHz, larger errors were seen at the shorter distances (figure 15). At 50 MHz, much smaller errors are seen at all distances (figures 16 and 17). At 101.5 MHz, larger errors were seen at the longer distances (figures 18 to 20).

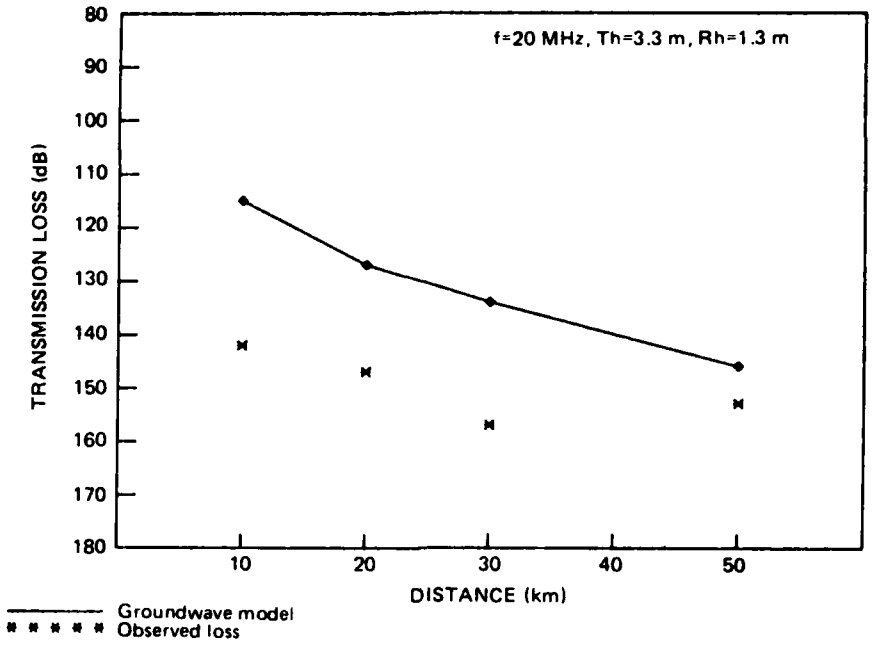

Figure 15. Colorado mountains median observed transmission-loss data compared to the GROUNDWAVE model as a function of distance, f=20 MHz, T_h=3.3 m, R_h=1.3 m.

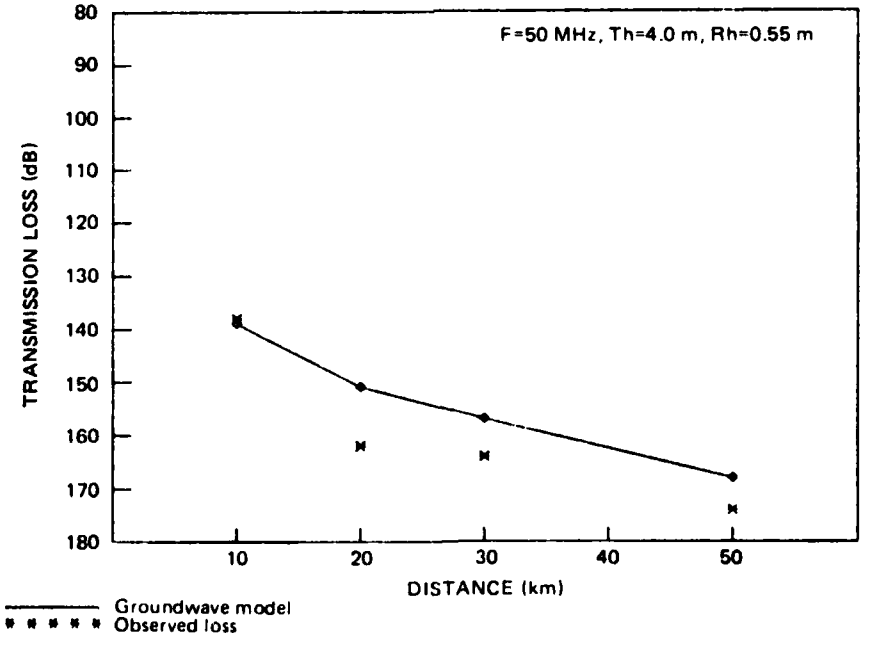

Figure 16. Colorado mountains median observed transmission-loss data compared to the GROUNDWAVE model as a function of distance, f=50 MHz, T_h=4.0 m, R_h=0.55 m.

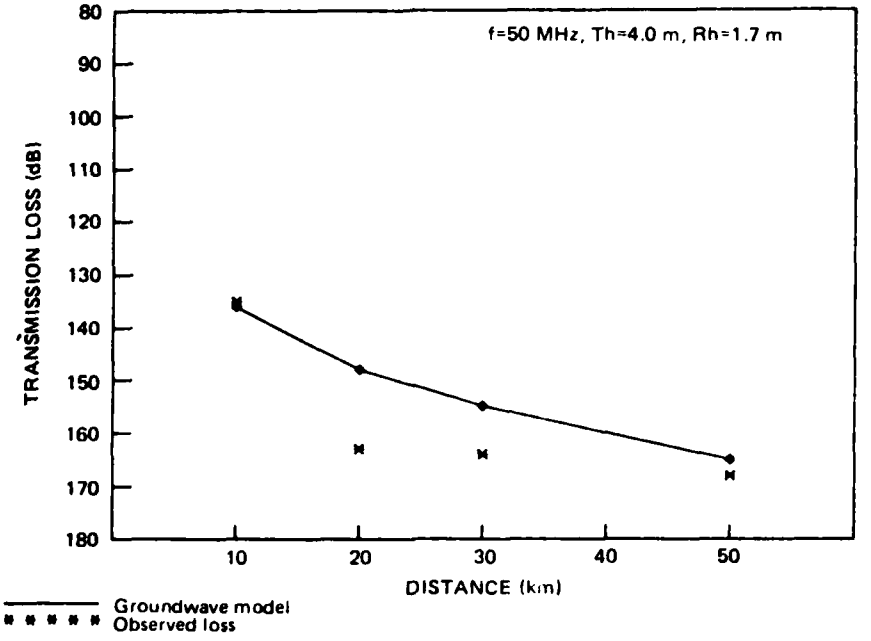

Figure 17. Colorado mountains median observed transmission-loss data compared to the GROUNDWAVE model as a function of distance, f=50 MHz, T_h=4.0 m, R_h=1.7 m.

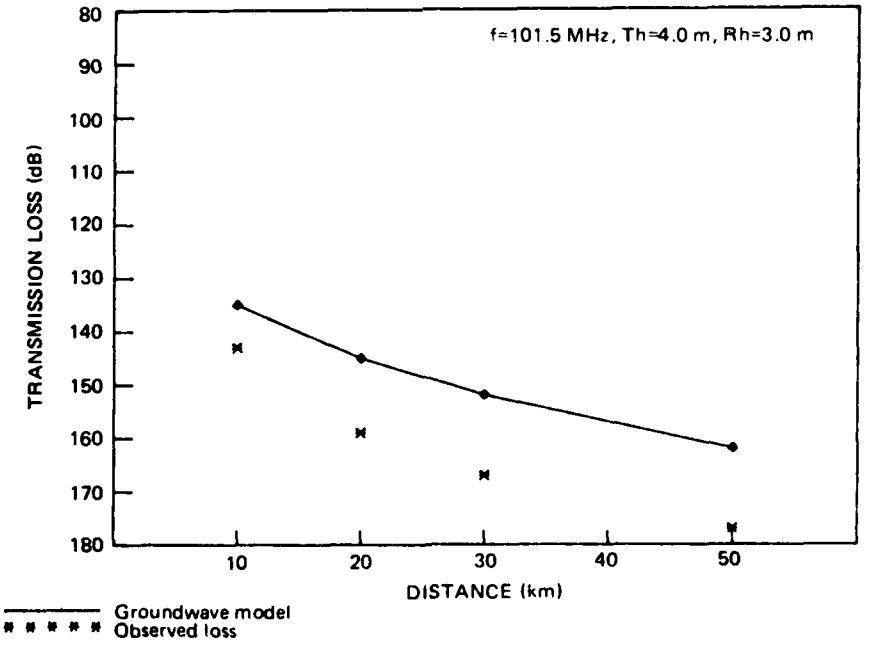

Figure 18. Colorado mountains median observed transmission-loss data compared to the GROUNDWAVE model as a function of distance, f=101.5 MHz, T_h=4.0 m, R_h=3.0 m.

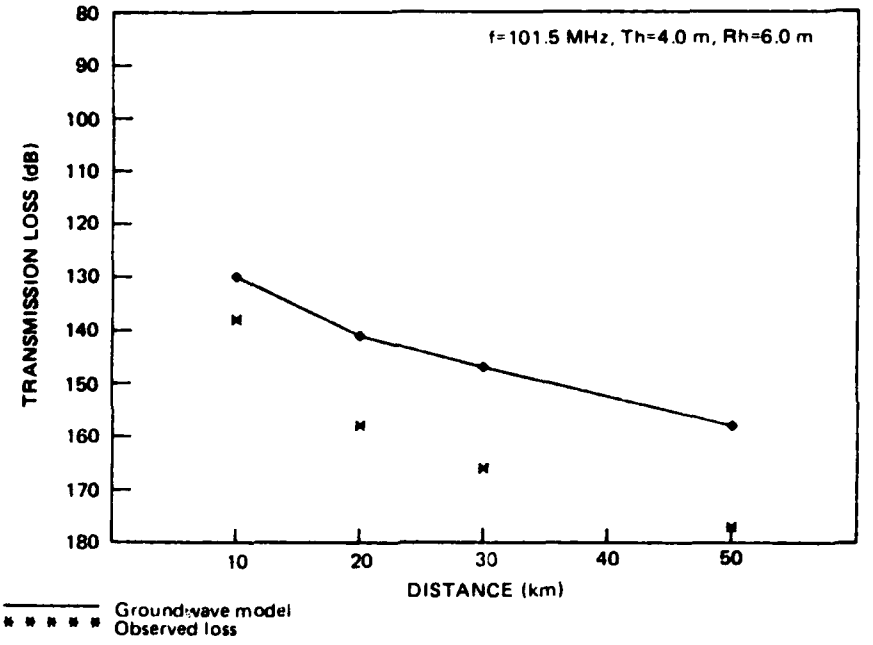

Figure 19. Colorado mountains median observed transmission-loss data compared to the GROUNDWAVE model as a function of distance, f=101.5 MHz, T_h=4.0 m, R_h=6.0 m.

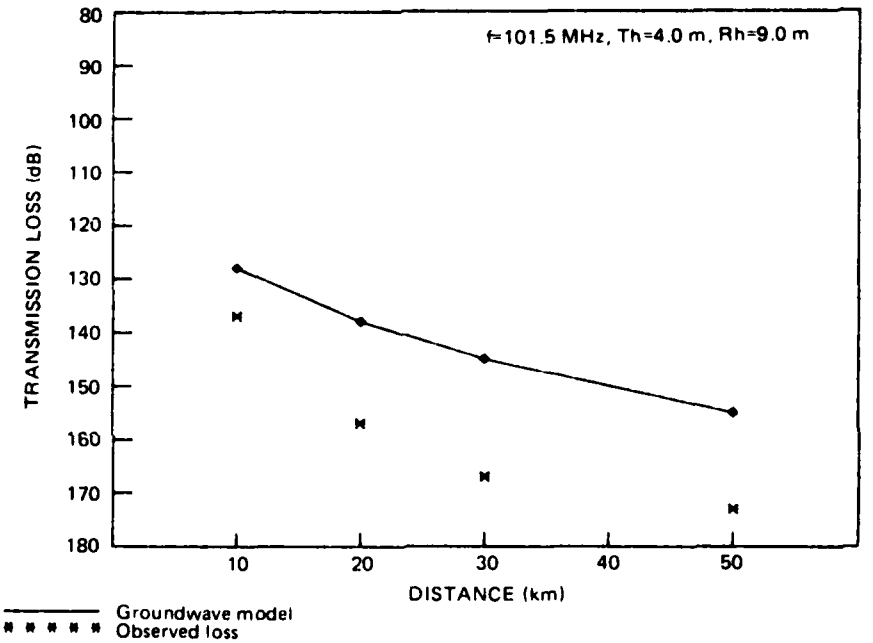

Figure 20. Colorado mountains median observed transmission-loss data compared to the GROUNDWAVE model as a function of distance, f=101.5 MHz, T_h=4.0 m, R_h=9.0 m.

5.3 OHIO HILLS PROPAGATION PATH

Transmission-loss measurements were made in northeastern Ohio over 255 paths at nominal distances of 10, 20, 30, and 50 km. Transmitter antenna heights ranged from 3.68 to 4.24 m and receiver antenna heights ranged from 1 to 9 m. Frequencies used were 20, 50, and 101.8 MHz.

In figure 21, median transmission-loss data for the Ohio hills tests and the GROUNDWAVE model results are plotted as a function of distance for a frequency of 20 MHz. Transmitter antenna height was 3.68 m and the receiver antenna height was 3.0 m. Model values are within the interdecile values at 30 and 50 km. The model underestimates the transmission loss with an average bias of +9.2 dB.

A new set of conditions is shown in figure 22. The frequency has increased to 50 MHz, transmitter antenna was raised to 4.24 m, and the receiver antenna was lowered to 1.0 m. Model values are within the interdecile ranges for 10 and 50 km distances only. The model overestimates the transmission loss for these conditions with an average bias of -10.0 dB.

Figure 23 shows comparison results for a receiver height of 3.0 m. Model values are within the interdecile ranges for all distances. The model still overestimates the transmission loss with an average bias of -7.7 dB.

The frequency was increased to 101.8 MHz and the transmitter antenna was lowered to 4.0 m for the set of data plotted in figure 24. Model values are within the interdecile ranges except at the 30 km distance. Transmission loss is overestimated, having an average bias of -7.0 dB.

The receiver antenna height was raised to 6 m and the resulting transmission-loss data for the Ohio hills is plotted in figure 25. GROUNDWAVE model values are within the interdecile ranges for all distances. The model now slightly underestimates the transmission loss with an average bias of +0.8 dB.

In figure 26 the model and observed data are compared with the receiving antenna raised to 9 m. Again, all model values are within the interdecile ranges. The model still slightly underestimates the transmission loss with an average bias of 0.3 dB.

The GROUNDWAVE model overestimated the transmission loss for three Ohio hills data sets (figures 22 to 24) and underestimated the transmission loss for three data sets (figures 21, 25, and 26). The overall average bias for all Ohio hills paths was small, -2.4 dB.

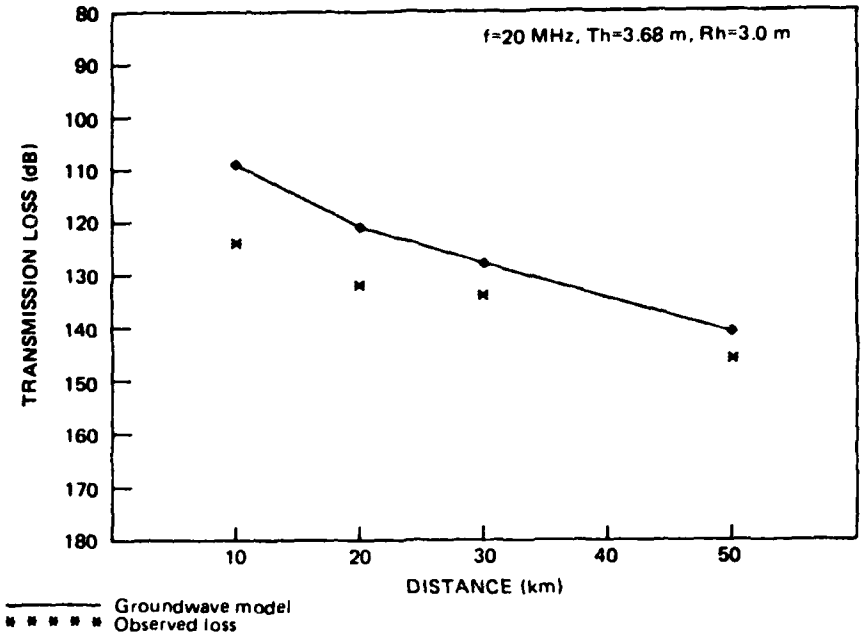

Figure 21. Ohio hills median observed transmission-loss data compared to the GROUNDWAVE model as a function of distance, f=20 MHz, T_h=3.68 m, R_h=3.0 m.

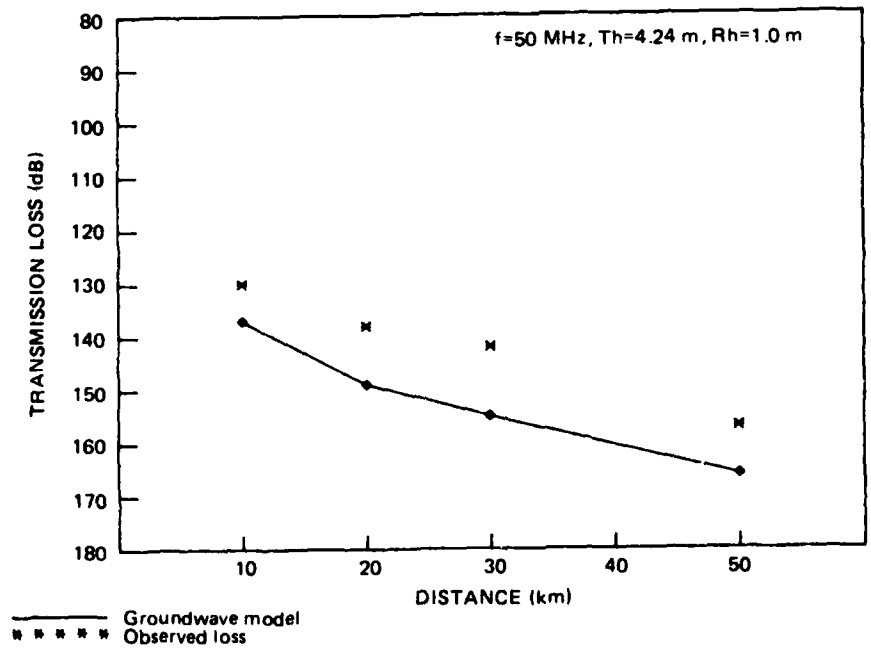

Figure 22. Ohio hills median observed transmission-loss data compared to the GROUNDWAVE model as a function of distance, f=50 MHz, T_h=4.24 m, R_h=1.0 m.

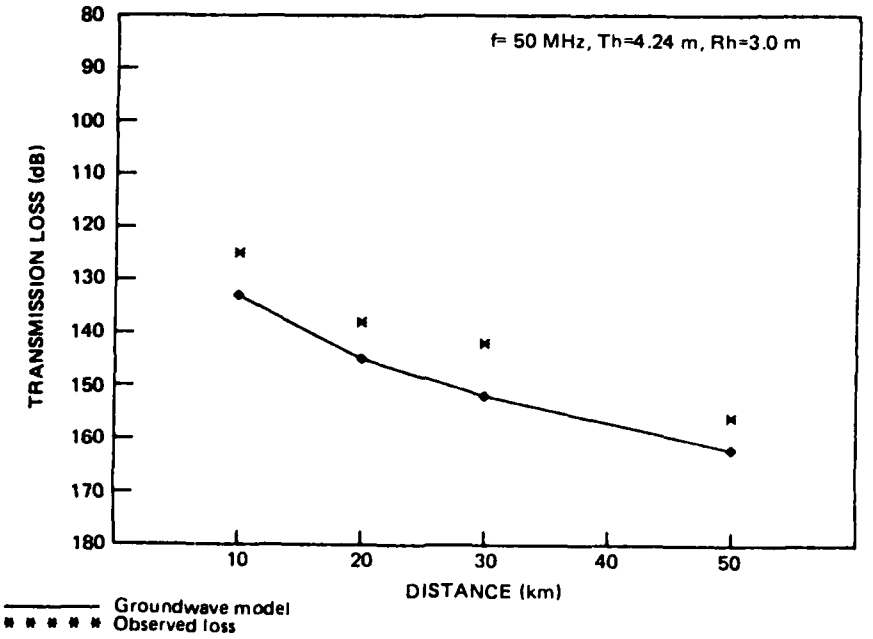

Figure 23. Ohio hills median observed transmission-loss data compared to the GROUNDWAVE model as a function of distance, f=50 MHz, T_h=4.24 m, R_h=3.0 m.

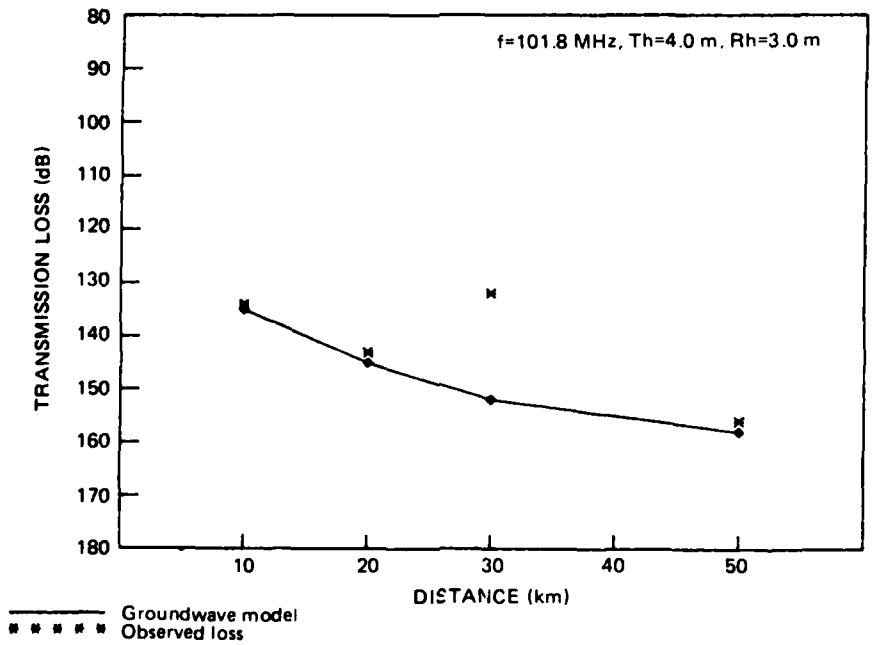

Figure 24. Ohio hills median observed transmission-loss data compared to the GROUNDWAVE model as a function of distance, f=101.8 MHz, T_h=4.0 m, R_h=3.0 m.

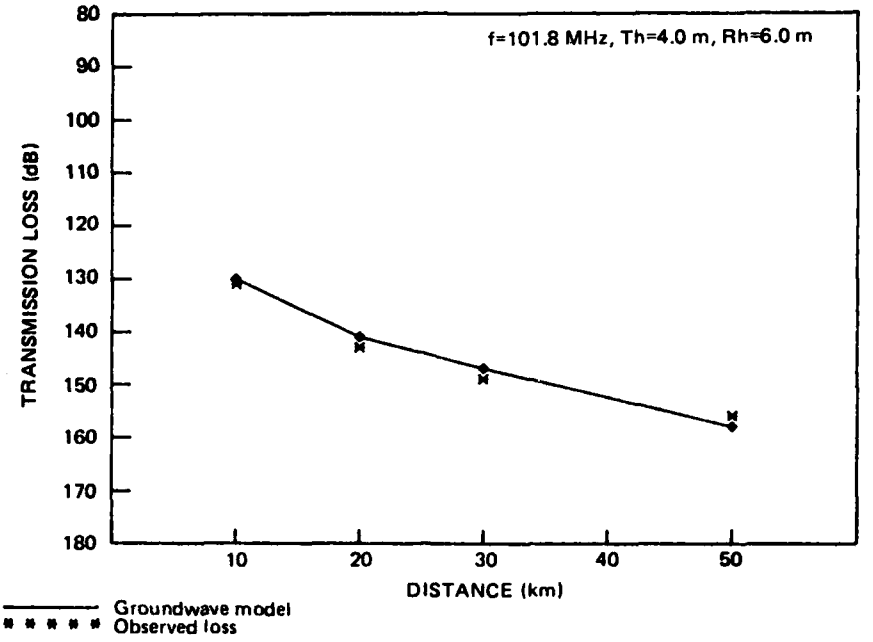

Figure 25. Ohio hills median observed transmission-loss data compared to the GROUNDWAVE model as a function of distance, f=101.8 MHz, T_h=4.0 m, R_h=6.0 m.

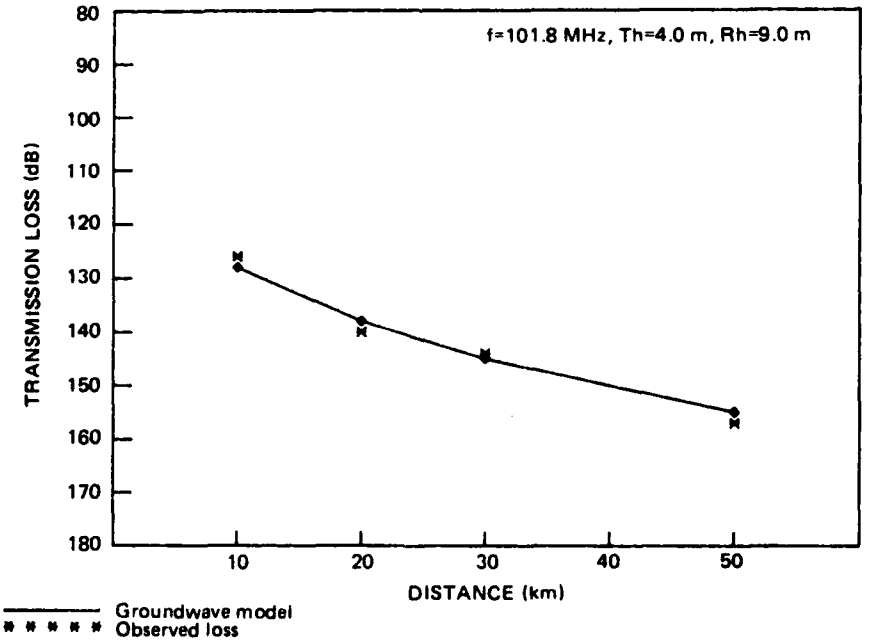

Figure 26. Ohio hills median observed transmission-loss data compared to the GROUNDWAVE model as a function of distance, f=101.8 MHz, T_h=4.0 m, R_h=9.0 m.

5.4 ERRORS AS A FUNCTION OF DISTANCE

In figure 27 GROUNDWAVE model bias is shown as a function of distance for the three different terrain types measured. No clear trend is seen, although there may be some increase in bias, some overestimation of transmission loss for Ohio hills and Colorado plains, and some underestimation for Colorado mountains for distances of 20 to 30 km.

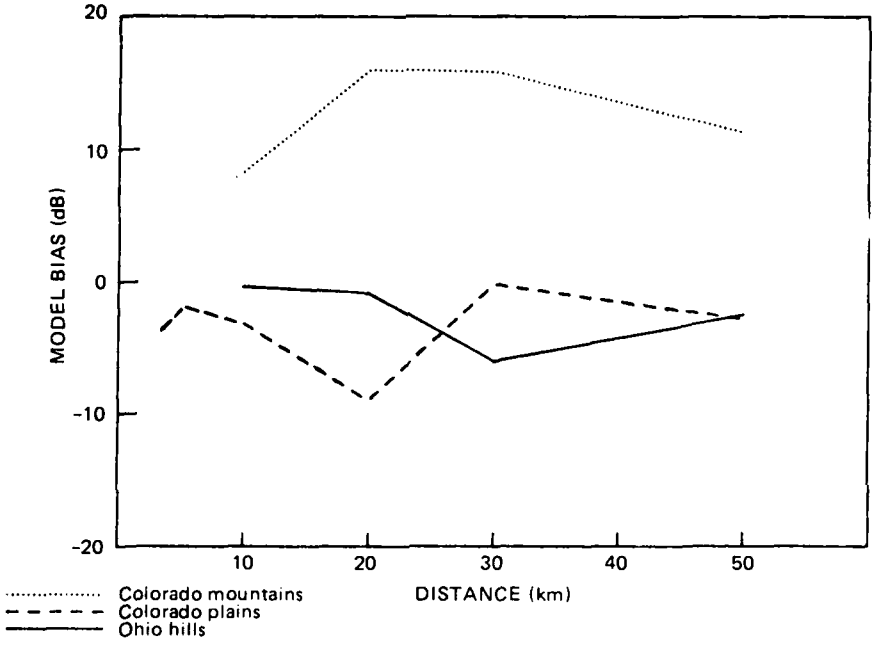

Figure 27. GROUNDWAVE model bias as a function of distance for three different terrain types.

5.5 ERRORS AS A FUNCTION OF FREQUENCY

In figure 28 GROUNDWAVE model bias is shown as a function of frequency for the three different terrain types measured. Again, no clear trend is seen, however there may be a slight trend to overestimate at 50 MHz and underestimate at 20 MHz. Also shown is an underestimation for the Colorado mountains at all frequencies, and some increase in bias, with overestimation for Ohio hills and Colorado plains at the higher frequencies.

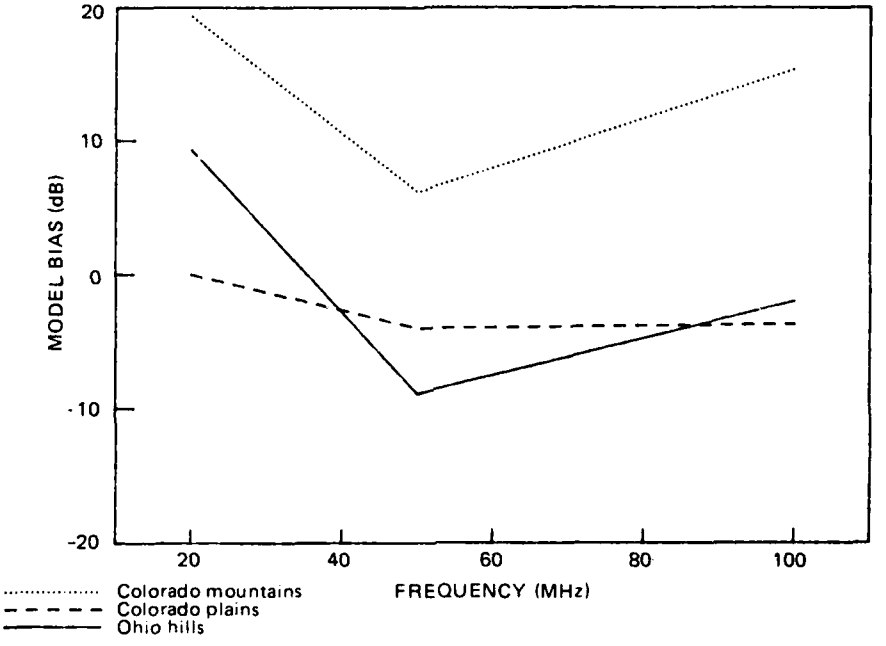

Figure 28. GROUNDWAVE model bias as a function of frequency for three different terrain types.

5.6 ERRORS AS A FUNCTION OF TERRAIN TYPE

Figure 29 shows GROUNDWAVE model bias as a function of terrain type. A clear trend is seen as mountain terrain transmission loss is underestimated by an average of +12.85 dB. Both hills and plains were overestimated by -2.4 dB and -3.18 dB, respectively. There is a trend toward underestimating the transmission loss as a terrain becomes more irregular.

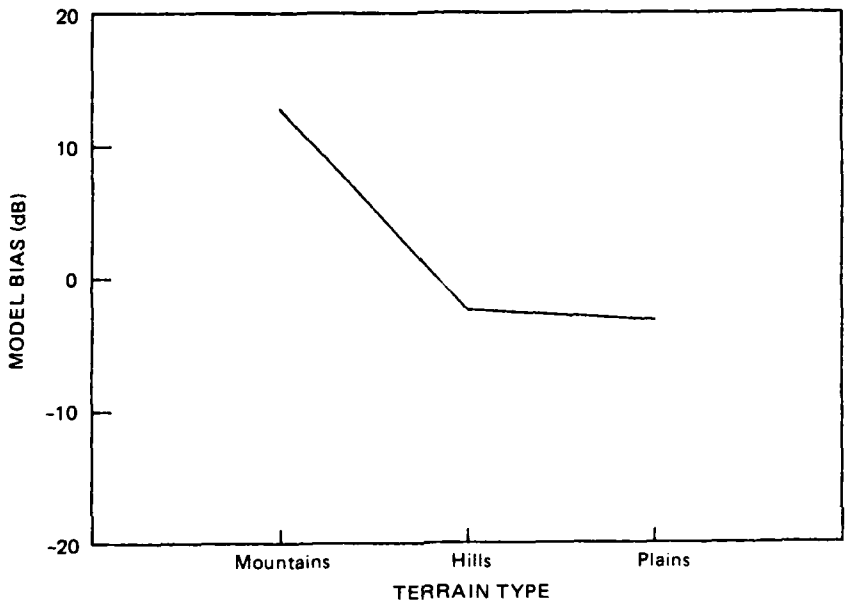

Figure 29. GROUNDWAVE model bias as a function of terrain type.

5.7 ERRORS AS A FUNCTION OF RECEIVER ANTENNA HEIGHT

In figure 30, GROUNDWAVE model bias is shown as a function of receiver antenna height. There is a tendency to overestimate at lower heights and to underestimate at higher antenna heights. The large variation in bias at 1.0 to 1.3 m is probably due to lack of data at these heights.

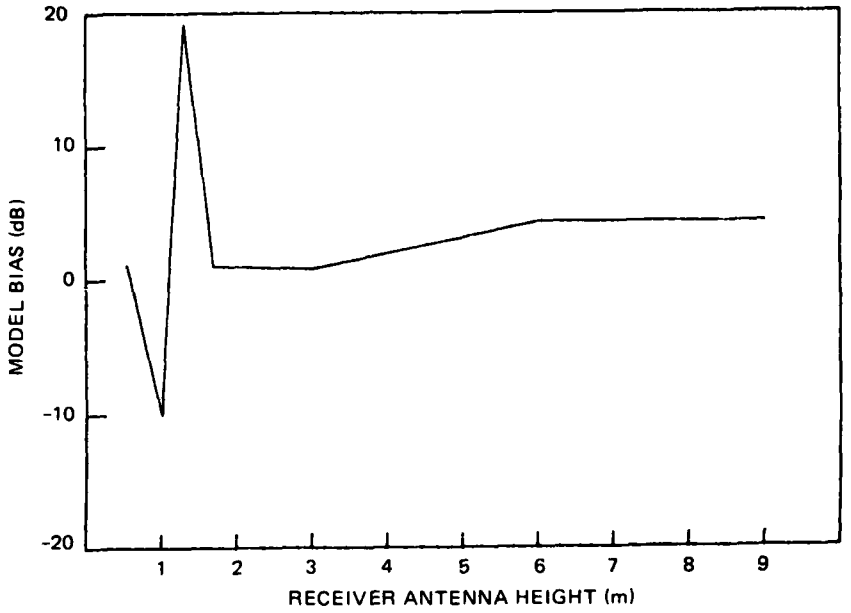

Figure 30. GROUNDWAVE model bias as a function of receiver antenna height.

5.8 ERRORS AS A FUNCTION OF THE EARTH'S SURFACE CHARACTERISTICS

The GROUNDWAVE model uses constant values of effective ground conductivity and effective ground relative dielectric constant for different frequencies in the calculation of transmission loss. The values are listed in table 2 for selected terrain categories. Hagn, Sifford, and Shepherd (1982) have shown graphically how conductivity and the dielectric constant vary as a function of frequency and terrain type. Effective ground relative dielectric constant is shown in figure 31 and effective ground conductivity is shown in figure 32. By using constant values for ground conductivity and dielectric constant in the GROUNDWAVE model, the possibility exists for substantial error in transmission-loss calculations as a function of frequency. To evaluate this error, GROUNDWAVE calculations were made using constant values in table 2 and then values from figures 31 and 32 for the frequency range 2 to 30 MHz.

Table 2. GROUNDWAVE model effective ground conductivity and relative dielectric constant for selected terrain categories.

Terrain Categories	Ground Conductivity mhos/m	Dielectric Constant
Marsh	0.110	30.0
Rich Agricultural	0.040	20.0
Medium hills	0.028	15.0
Mountains	0.015	6.0
Flat desert	0.011	4.0

Transmission-loss values calculated using the constants were subtracted from values calculated using figures 31 and 32. The resulting difference as a function of frequency is plotted in figures 33 and 34. Figure 33 shows the possible error as a function of frequency for desert, mountainous, and hilly terrain. As can be seen, the model underestimates the transmission loss with significant error at the lower frequencies for all three terrain types. Figure 34 shows the possible error as a function of frequency for rich agricultural and marsh terrain. In this test, the model slightly overestimated the transmission loss with greater error at the higher frequencies.

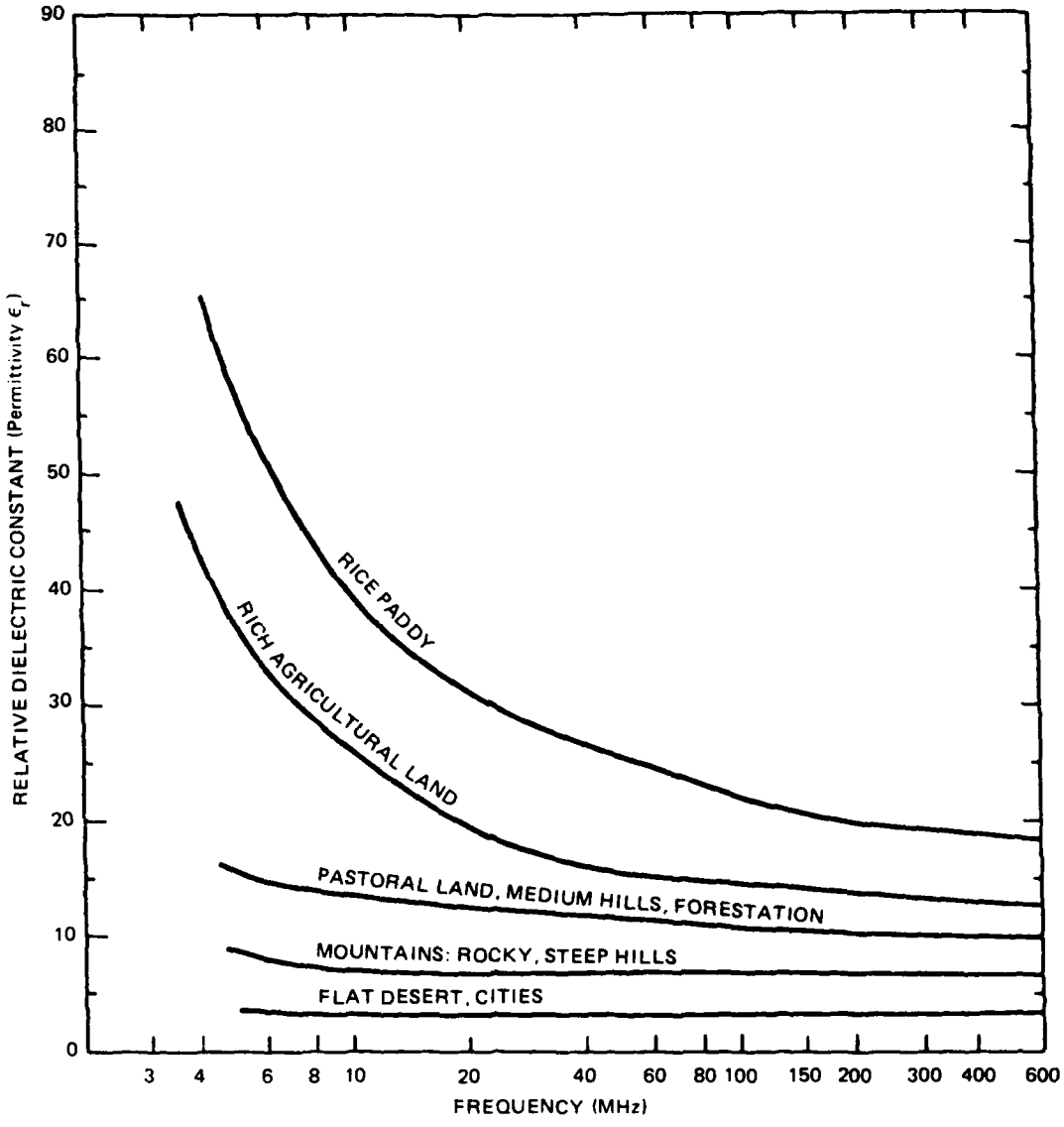

Figure 31. Effective ground relative dielectric constant versus frequency for selected terrain categories.

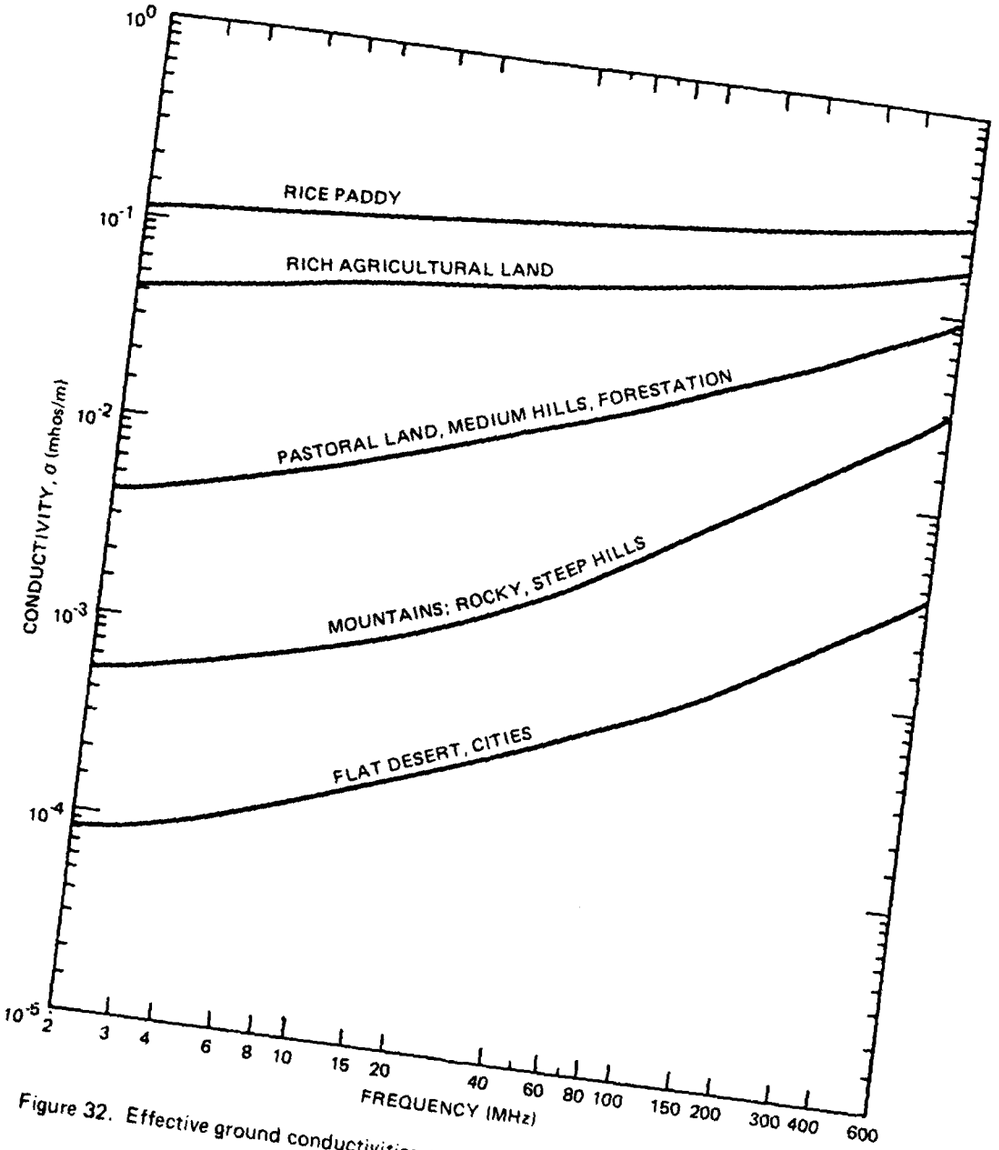

Figure 32. Effective ground conductivities versus frequency for selected terrain categories.

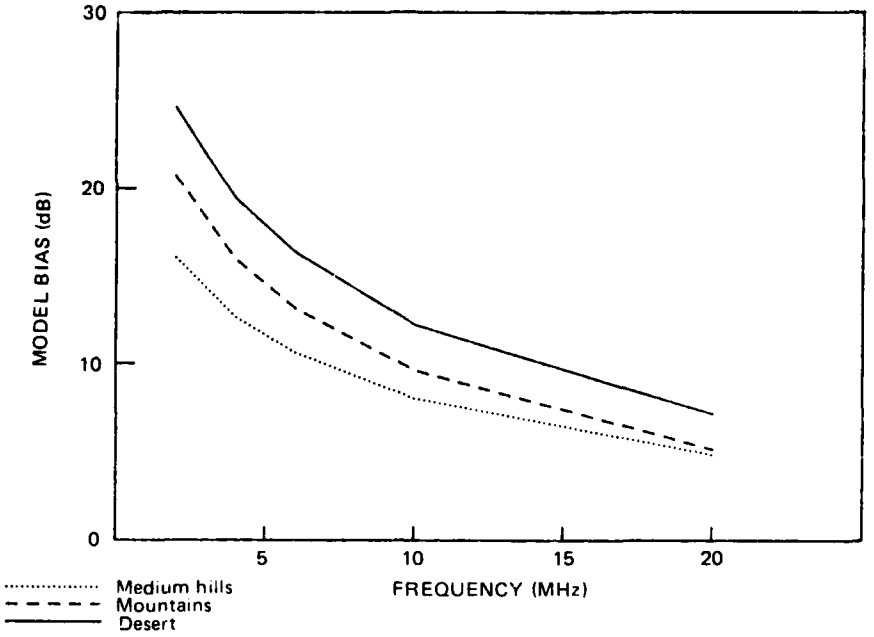

Figure 33. Possible GROUNDWAVE transmission-loss error as a function of frequency for desert, mountainous, and hilly terrain.

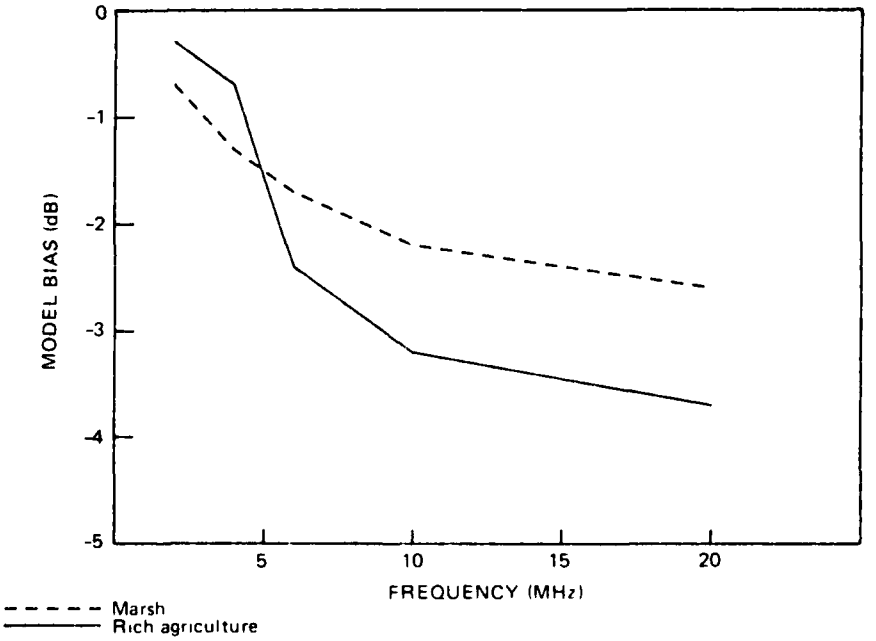

Figure 34. Possible GROUNDWAVE transmission-loss error as a function of frequency for rich agricultural and marsh terrain.

6.0 DISCUSSION OF ACCURACY OVER SEA PATHS

A comparison was made of measurements made by Hansen (1977) and predictions using GROUNDWAVE. The transmitter was located on Point Loma in San Diego at an elevation of 29.57 m near the edge of the sea bluffs. The receiver was located at Point Mugu at an elevation of approximately 3.05 m above sea level. This over-ocean propagation experiment was performed for a 1-month period from 29 May to 26 June 1974. Measured received signal power was recorded about twice a day. Table 3 presents the average transmission loss measured by Hansen and the lower and upper sigma points of his measurements. A total 36 measurements were used by Hansen as a basis for these results.

Figure 35 shows the results of this comparison. The transmission losses from GROUNDWAVE have been increased by 6 dB to account for the approximately 6 dB difference in gain existing at take-off angle 0 degree between sky-wave and ground-wave receive antenna patterns. First, the transmission losses estimated by GROUNDWAVE were nearly always larger than those measured except in the range 12 MHz to 16MHz where sea state affected the measured results. In this range the results predicted for sea state 2 were close to those measured. Beyond 18 MHz the measured results and predicted results depart considerably with the measured results being much less. These results are similar to that observed by Hansen (1977) between the measured results and those obtained for four-thirds earth, effective earth-radius representation for the atmosphere in the prediction of the theoretical results.

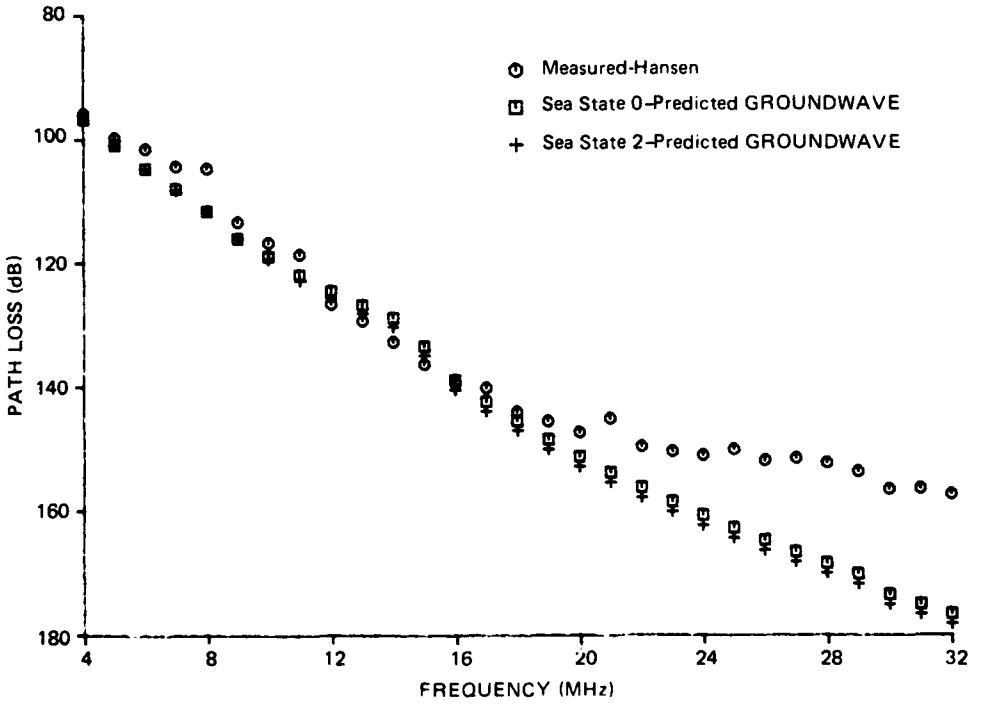

Figure 35. GROUNDWAVE transmission-loss for over sea case as a function of frequency and sea state.

Table 3. Measured ground-wave transmission loss over sea due to Hansen (1977).

Frequency (MHz)	Average loss (dB)	Lower and Upper Sigma values of loss (dB)		
4.0	95.828	95.227	to	96.058
5.0	99.697	98.790	to	100.085
6.0	101.490	100.397	to	101.937
7.0	104.403	103.666	to	104.742
8.0	104.730	104.052	to	105.323
9.0	113.380	112.453	to	114.115
10.0	116.735	115.771	to	117.140
11.0	118.670	117.794	to	118.796
12.0	126.645	125.707	to	127.051
13.0	129.372	128.243	to	129.808
14.0	132.753	131.856	to	133.370
15.0	136.319	135.421	to	137.303
16.0	139.326	138.175	to	140.082
17.0	140.208	139.561	to	141.199
18.0	144.171	143.516	to	145.007
19.0	145.567	144.173	to	145.469
20.0	147.361	145.707	to	147.591
21.0	145.142	143.780	to	145.077
22.0	149.665	147.513	to	147.562
23.0	150.454	147.007	to	148.596
24.0	151.081	147.949	to	150.373
25.0	150.121	148.439	to	150.957
26.0	151.937	150.363	to	152.880
27.0	151.608	150.038	to	153.631
28.0	152.327	150.911	to	154.285
29.0	153.724	152.103	to	155.819
30.0	156.543	154.712	to	157.891
31.0	156.471	154.755	to	157.934
32.0	157.354	156.169	to	158.514

7.0 CONCLUSIONS AND RECOMMENDATIONS

The GROUNDWAVE model was compared to 84 surface-wave measurements made at frequencies of 20, 50, and 101.5 MHz for three different types of land terrain. The model was evaluated for distances from 3 to 50 km, transmitter antenna heights from 3.3 to 4.24 m and receiver antenna heights from 0.55 to 9.0 m. The overall average measured transmission loss was 144 dB with an average interdecile range of ±11 dB. The overall calculated transmission loss was 141 dB, well within the interdecile range.

When the GROUNDWAVE model was examined as a function of terrain type, a trend toward underestimating the transmission loss as the land terrain became more irregular was apparent. Agreement was very good for Colorado plains and Ohio hills data with the model overestimating transmission loss by 3.2 and 2.4 dB, respectively. For the Colorado mountains, the agreement was not as good with the model underestimating transmission loss by 12.9 dB. No clear trends in the error results are seen for model evaluations as a function of distance or frequency. There is a tendency to overestimate the losses at lower receiver antenna heights (i.e., less than 1 m) and to underestimate at higher heights.

GROUNDWAVE model error was also evaluated as a function of input effective ground conductivity and effective ground relative dielectric constant over land. When ground constants were held constant in the frequency range 2 to 20 MHz, the model underestimated the transmission loss by an average of 13.1 dB for desert, mountainous, and hilly terrain. Error decreased from about 20 dB at 2.0 MHz to 5 dB at 20.0 MHz. For rich agricultural and marsh terrain, the GROUNDWAVE model overestimated the transmission loss by an average of 1.9 dB.

GROUNDWAVE was also evaluated as a function of frequency for an over ocean path. It was found for the case studied that the transmission loss was severely overestimated for frequencies greater than 18 MHz. This error is due to the likelihood that GROUNDWAVE has no way to change the atmosphere for calculations that are made.

As a result of this study, the following recommendations are made:

1. that the frequency-dependent curves representing the ground conductivity and effective ground relative dielectric constant be incorporated into the GROUNDWAVE model;

2. that the accuracy of the modified GROUNDWAVE model be assessed for the three different types of terrain used here;

3. that the surface-wave model in GROUNDWAVE be modified for use within nonstandard atmospheres;

4. that as a separate comparison, determine the accuracy of the surface-wave model in the Army PROPHET Evaluation System (APES) where these same curves have been implemented in EPM-73;

5. that the surface-wave model in APES be considered for use when surface roughness (i.e., no winds) is of no concern, particularly if it should prove to be more accurate.

8.0 REFERENCES

Barrick, D.E., Jan 1970. Battelle Memorial Institute Res. Rep., AD 865 840, "Theory of Ground-Wave Propagation Across a Rough Sea at Dekameter Wavelengths."

Barrick, D.E., May 1971a. "Theory of HF and VHF Propagation Across the Rough Sea, 1, the Effective Surface Impedance for a Slightly Rough Highly Conducting Medium at Grazing Incidence," *Radio Science*, vol. 6, p. 517-526.

Barrick, D.E., May 1971b. "Theory of HF and VHF Propagation Across the Rough Sea, 2, Application to HF and VHF Propagation Above the Sea," *Radio Science*, vol. 6, p. 527-533.

Berry, L.A, Jan 1978. Office of Telecommunications Report 78-247, "User's Guide to Low-frequency Radio Coverage Programs."

Booker, H.G. and R. Lugananni, Nov 1978. Naval Ocean Systems Center TR 208, "HF Channel Simulator for Wideband Signals."

Bullington, K., Oct 1947. "Radio Propagation at Frequencies above 30 Megacycles", *Proc. IRE*, vol. 35, p. 1122-1136.

Electromagnetic Compatibility Analysis Center, Oct 1975. "ECAC Calculator Program #11-4, Ground-Wave Path-Loss Model."

Hagn, G.H., B.M. Sifford, and R.A. Shepard, May 1982. SRI International final report SRI Project, 3603, contract NT-81-RC-1601, "The SRICOM Probabilistic Model of Communication System Performance."

Hansen, P., May-June 1977. "Measurements of Basic Transmission Loss for HF Ground-Wave Propagation Over Sea Water," Radio Science, vol. 12, p. 397-404.

Langley, A.G. and R.K. Reasoner, January 1970. Environmental Sciences Services Administration TR ERL 148-ITS 97, "Comparison of Propagation Measurements with Predicted Values in the 0 to 10,000 MHz Range."

Levine, P.H., Sep 1978. Megatek Informal Report, "Coverage Estimates in Tactical LPI Communications Systems Analysis."

Lustgarten, M.N. and J.A. Madison, Aug 1977. "An Empirical Propagation Model (EPM-73)," *IEEE Tran. Electromagnatic. Compat.*, vol. EMC-19, No. 3.

MEGATEK Corporation, Apr 1977. Memorandum ser SAN: 0398:PHL to NOSC, Subject: MINIMUF II and MINISURF.

Norton, K.A., Oct 1936. "The Propagation of Radio Waves Over the Surface of the Earth and in the Upper Atmosphere, 1, Ground-Wave Propagation from Short Antennas," *Proc. IRE*, vol. 24, p. 1367-1387.

Norton, K.A., Sep 1937a. "The Propagation of Radio Waves over the Surface of the Earth in the Upper Atmosphere, 2, the Propagation from Vertical, Horizontal and Loop Antennas over a Plane Earth of Finite Conductivity," *Proc. IRE*, vol. 25, p. 1203-1236, Sep 1937a.

Norton, K.A., Sep 1937b. "The Physical Reality of Space and Surface Waves in the Radiation Field of Radio Antennas," *Proc. IRE*, vol. 25, p. 1192-1202.

Norton, K.A., Dec 1941. "The Calculation of Ground Wave Field Intensity over a Finitely Conducting Spherical Earth," *Proc. IRE*, vol. 29, p. 623-639.

Norton, K.A., 1957. National Bureau of Standards Rep. 5092, "Transmission Loss in Radio Propagation," Part 2.

Pappert, R.A. and C.L. Goodhart, Sep-Oct 1979. "A Numerical Study of Tropospheric Ducting at HF," *Radio Science*, vol. 14, p. 803-813.

Sailors, D.B., W.K. Moision, and T.N. Roy, Dec 1983. Naval Ocean Systems Center TD 642, "The New U.S. Army PROPHET Evaluation System (APES) Models."

Sommerfeld, A., May 1909. "The Propagation of Waves in Wireless Telegraphy," *Am. Physik*, vol. 28, p. 665-736.

Wait, J.R., 1964. "Electromagnetic Surface Waves," *Advances in Radio Research*, vol. 1, p. 157-217.

Wong, J., J.R. Rossiter, G.R. Olhoeft, and D.W. Strongway, 1977. "Permafrost: Electrical Properties of the Active Layer Measured in Situ," *Can J. Earth Science.*, vol. 14, p. 582-586.

APPENDIX A

FORTRAN SURFACE-WAVE PROGRAM

The listing of the GROUNDWAVE model that follows is written in FORTRAN 77 for the Hewlett-Packard (HP) 9050 computer.

```
      subroutine gdwave(rlat,rlon,ie,pt,xlg)
cp
c      subroutine gdwave
c
c        call gdwave(rlat,rlon,ie,pt,xlg)
c
c        this routine determines which of the ground wave model should
c        be used in the analysis.  the analysis type is a function of
c        polarization, terrain, transmitter and receiver heights, and
c        frequency.  rlat,rlon are the receiver lat/lon (radians)
c        and are used for atmospheric noise calculations.
c
c        subroutines and functions used: ecac
c                                        epm73
c                                        gndbl
c                                        gndlev
c                                        mmnois
c                                        noise
c                                        sealos
c
c        common blocks:  sysdat
c
cz
c
      integer itime(6)
      include 'sysdat.inc'
      equivalence(itime(1),misc(1))
c
      hite1=thite
      hite2=rhite
      freq=tfreq
      xloss=0.0
c
c   check to see which model to use
c
c   if path over sea and antennas vertical & < 10 meters, keep
c   checking, otherwise use either epm73 or ecac.
c
      if(ter .ne. 'se' .or. (hite1 .gt. 10..or.hite2 .gt. 10.)
     &     .or. polar .eq. 'h'    )  go to 1000
c
c   if freq less than 30 mhz, use the booker/lugannani model
c
      if(freq .gt. 30.) go to 2000
      if(freq .le. 3.0) go to 1500
      call gndbl(freq,range,xlg)

      go to 8000
c
c   if freq greater than 30 mhz, use epm73
c
1000  if(freq.lt.30.) go to 1500
      call epm73(freq,hite1,hite2,range,polar,ter,xlg)
      go to 8000
c
c   freq must be less than 30 mhz, use ecac
c
1500  call ecac(freq,range,cond,epslon,hite1,hite2,polar,xlg,ie)
```

```
      go to 8000
c
c   if freq less than 100 mhz, first try levine model
c   if freq greater than 40 mhz, epm73 is more accurate
c
2000  if(freq.lt.100.) call gndlev(freq,range,xlg)
      if(freq.ge.40.) call epm73(freq,hite1,hite2,range,polar,ter,xlg)
c
c   basic groundwave loss calculated.  compute the rest of the stuff
c
8000  continue
c
c   check to see whether seastate loss should be included
c
      if(wind .gt. 5. .and. epslon .gt. 40. .and. polar .eq. 'v')
     &    call sealos(wind,freq,range,xloss)
      if(xloss .gt. 0.)xlg=xlg+xloss
c
c   call the noise model appropriate to conditions
c
      if(iatmos.ne.'y') call mmnois(freq,nse,fa)
      if(iatmos.eq.'y') call noise(freq,nse,fa,rlat,rlon,itime)
c
c
c   required power of transmission:
c      pt=lg-fa+10alog10(b)+rmd-124.
c
      pt= xlg+fa+10.*alog10(bwidth)+signse-124.
      pt=10.**((pt-30.)/10.)
c
900   return
      end
```

```
      subroutine ecac(f,d,sigma,er,h1,h2,polar,loss,ierr)
cp
c      subroutine ecac
c
c        call ecac(f,d,sigma,er,h1,h2,polar,loss,ierr)
c
c        this routine is designed to compute the groundwave transmission
c        loss over a smooth, spherical earth for vertically and horizont
c        polarized signals between 1-30 mhz.  this model uses a theoreti
c        formulation that differenciates between distances short enough
c        assume planar earth, and longer distances where the earth's cur
c        becomes important.  the parameters required are frequency (f),
c        distance (d), surface conductivity in mhos/m (sig), surface die
c        constant (er), antenna heights (h1 and h2), and polarization (p
c        this routine returns a zero if the calculation was okay otherwi
c        a one will be returned
c
c        subroutines and functions used:  beta0
c                                         gwdist
c                                         vsea
c
c        common blocks:  none
c
cz
      character*1 polar
      real loss,lfs,m
      data pi/3.14157/
c
c   change conductivity to mmhos
      sig=1000.*sigma
c
c   set error flag
      ierr=0
c
c
c   free space loss
c
       lfs=20.*alog10(2.*pi*d*f/0.3)
c
c
c   if vertical over sea, with f<15.5 do seperate calc
c
      vs=0.
      if(polar .eq. 'v' .and. f .le. 15.5
     &   .and. sig .gt. 3000. .and. er .gt. 50.)vs=1.
      if(vs .eq. 1.)call vsea(f,d,sig,er,h1,h2,lfs,loss,ierr)
c   add factor to get ccir to berrik values(3.52 db)
      if(vs .eq. 1)loss=loss+3.52
      if(vs .eq. 1.)return
c
c
c   otherwise find dfsm and dc to determine short or long range
c
      dc=150./(f**0.5305)
      dfsm=gwdist(h1,h2,f,sig,er,polar)
c
      if(dfsm .gt. 2.*dc)ierr=1
c
```

```
c
      if(d .lt. dfsm/2.)loss=lfs-6.0
      if(d .ge. dfsm/2. .and. d .le. dc)loss=lfs+20.*alog10(d/dfsm)
c
c   if d < dc then return because did short range
c
      if(d .le. dc)return
c
c   longer range
c
      if(polar .eq. 'h')b0=1.607
      if(polar .eq. 'v')b0=beta0(f,sig,er)
c
c      calculate the ground wave loss slope
c
      m=0.0572*b0*f**(1./3.) - 0.01
c
c
      loss=lfs + 20.0*alog10(dc/dfsm) + m*(d-dc)
c
c   add the factor to get ccir(ecac) to barrik curves (3.52db)
      loss=loss+3.52
c
      return
      end
```

```
      subroutine epm73(f,h1,h2,d,polar,terain,lb)
cp
c      subroutine epm73
c
c        call epm73(f,h1,h2,d,polar,terain,lb)
c
c        epm73 (lustgarten/madison empirical propagation modes) is
c        similiar to ecac in including direct ray, reflected ray,
c        and the surface wave, but also includes troposcatter effects
c        at greater distances.  internally this model is logically
c        seperated into two sections, hihl and lowhl.  the parameters
c        required for this model are the frequency (f), the antenna
c        heights (h1 and h2), the distance (d), the polarization
c        (polar), and the terrain (terain).  this routine returns the
c        maximum loss calculated by either hihl or lowhl.
c
c        subroutines and functions used:  lowhl
c                                         hihl
c
c        common blocks:  none
c
cz
c
      real lb,lbl,lbh
      character*1 polar
      character*2 terain
c
      lb=0.
      if(f .lt. 30.  .or.  f .gt. 1000.)return
c
      call lowhl(f,h1,h2,d,polar,terain,lbl)
      call hihl (f,h1,h2,d,polar,terain,lbh)
c
      lb=amax1(lbl,lbh)
c
      return
      end
```

```
      subroutine gndbl (freq,range,lg)
cp
c      subroutine gndbl
c
c        call gndbl(freq,range,lg)
c
c        this model calculates the ground loss (lg) using the
c        lugannani and booker model.  these calculations are
c        performed for an antenna at the sea surface using
c        vertical polarized signals.  this model is extremely
c        accurate when the frequency is between 2 and 30 mhz
c        but it degrades rapidly outside that range.  the
c        parameters required for this routine are the frequency
c        (freq) and the distance (range).
c
c        subroutines and functions used:  none
c
c        common blocks:  none
c
cz
      real lg
c
c
c   groundwave loss, lg (lugannani and booker model)
c   for frequencies below 30mhz
c
      c1=1.78e-4*(freq**2.58)*exp(-1.4e-8*freq**5.)
      c2=1.83*freq**(-0.243)
       if(freq .le. 30.)lg= 20.*alog10((6.28314/0.3)*range*freq)
     &     + c1 * range**c2
c
      if(freq .gt. 30.)lg=0.
c
c
      return
      end
```

```
      subroutine gndlev (freq,range,lg)
cp
c      subroutine gndlev
c
c        call gndlev(freq,range,lg)
c
c        this model calculates the groundwave loss (lg) using
c        the levine method.  the accuracy of the result is not
c        as good asa the bl model for 2-30 mhz but it is gocd
c        for up to 100 mhz.  the input required for this model
c        is the frequency (freq) and the distance (range).
c
c        subroutines and functions used:  none
c
c        common blocks:  none
c
cz
      real lg
c
      a=1.45*exp(-freq/500.)
      b=(range/140.)**(exp(-0.008*(freq-3.)))
c
      lg=20.*alog10((6.28314/0.3)*range*freq)
     &   + a*b*freq
c
      return
      end
```

```
      subroutine mmnois (frq, nse, fam)
cp
c     subroutine mmnois
c
c       call mmnois (frq, nse, fam)
c
c       this routine uses the ccir and nosc noise models to estimate
c       the noise media (nse) vs the frequency (frq).  the types of
c       noise models permitted are shipboard (sh), business (bu),
c       residential (re), rural (ru), quiet rural (qr), and quasi-
c       minimum (qm).  this subroutine calculates only manmade noise
c       and is used in lieu of the rest of the routines in this lib-
c       rary when atmospheric noise is not desired.
c       the noise power fam is in db relative to ktb.
c
c       subroutines and functions used:  none
c
c       common blocks:  none
c
cz
c
      character*2 nse
c
c   default to qm if nse has not been set
c
      fam=-27.5*alog10(frq) + 60.
c
      if(nse .eq. 'sh')fam=-27.7*alog10(frq) + 76.8
      if(nse .eq. 'ur')fam=-27.7*alog10(frq) + 76.8
      if(nse .eq. 'bu')fam=-27.7*alog10(frq) + 76.8
      if(nse .eq. 're')fam=-27.7*alog10(frq) + 72.5
      if(nse .eq. 'ru')fam=-27.7*alog10(frq) + 67.2
      if(nse .eq. 'qr')fam=-28.6*alog10(frq) + 53.6
      if(nse .eq. 'qm')fam=-27.5*alog10(frq) + 60.0
c
c
c   calculate galactic noise if frequency above 10mhz
c
      if(frq .lt. 10.) go to 999
      ga=-23.0*alog10(frq) + 52.0
c
      if(ga .gt. fam) fam=ga
c
999   return
      end
```

```
      subroutine noise (f,type,xrnse,rlat,rlon,itime)
cp
c      subroutine noise
c
c        this routine uses the ccir and nosc noise models to estimate
c        atmospheric, galactic, and man-made noise
c
c        subroutines and functions used:  evutan
c                                         genfam
c                                         xinter
c
c        common blocks: nseb
c                       nsecal
c                       nsepar
c
c        parameters:
c           f       frequency(mhz)
c           type    man-made noise type. the types permitted are
c                   shipboard(sh),business(bu),residential(re),
c                   rural(ru), quiet rural(qr), and quasi-minimum(qm)
c           xrnse   calculated noise relative to ktb
c           rlat    receiver latitude, radians
c           rlon    receiver longitude, radians, positive west of 0 deg.
c           itime   month,day,hour(ut),min,second
c           gnoslm  lower frequency limit galactic noise
c           nnum    index to be set to zero in calling program for
c                   first call for a receive site for a season
c           anox    1 mhz atmospheric noise(ktb) for a receive site
c                   for each time block for a season
c
c        note: as currently programmed, shipboard noise and business man
-
c              made are the same.
c              gnos should be called whenever a new sunspot number or a
c              month is input to calling program.
c              noisdt should be called whenever a new season has been
c              determined by gnos.
c              common /nsecal/ determines if a new 1mhz noise need be
c              calculated.  if 0, then start from scratch.  if 1, then
c              it has been determined by the calling program that nothin
g
c              significant has changed, and only the frequency dependenc
e
c              for f need be recomputed.
c
cz
      character*2  type
      integer      itime(6)
      real         ltime
      common /nseb/ clg,clt,dt(11,7,6),gamma(6),num,nh,maxg
      common /nsecal/ justfr
      common /nsepar/gnoslm,nnum,anox(6)
c
      data ifirst / 0 /, twopi /6.2831853/
c
c   has just the frequency changed?
c
      if( ifirst.ne.0 .and. justfr.ne.0 ) go to 1000
```

```
c
c   atmospheric noise
c
      num=nnum
      clt=rlat
      clg=twopi-rlon
      if(rlon .lt. 0.0) clg=abs(rlon)
      if(num .ne. 0) go to 15
      nh=5
      maxg=7
      call evutan
      do 12 it=1,6
12    anox(it)=gamma(it)
      nnum=1
c     return
15    continue
      utime=float(itime(3))+(float(itime(4))/60.0)
      if(utime .ge. 24.0) utime=utime-24.0
      call xinter(utime,2,ntb,ntx,abct)
      anos=anox(ntb)+(anox(ntx)-anox(ntb))*abct
      ltime=utime-(rlon/0.261799388)
      if(ltime .ge. 24.0) ltime=ltime-24.0
      if(ltime .lt. 0.0) ltime=ltime+24.0
      ifirst = 1
c
1000  call xinter(ltime,1,ntb,ntx,abct)
      call genfam(rlat,ntb,f,anos,atno,du,dl,sigu,sigl,sigm)
      call genfam(rlat,ntx,f,anos,atnx,dux,dlx,sigux,siglx,sigmx)
      atmno=atno+(atnx-atno)*abct
      dua=du+(dux-du)*abct
      dla=dl+(dlx-dl)*abct
      sma=sigm+(sigmx-sigm)*abct
      sua=sigu+(sigux-sigu)*abct
      sla=sigl+(siglx-sigl)*abct
c
c   man-made noise
c
c   default to qm if type has not been set
c
      xnoise=-27.5*alog10(f) + 60.
c
      if(type .eq. 'sh')xnoise=-27.7*alog10(f) + 76.8
      if(type .eq. 'bu')xnoise=-27.7*alog10(f) + 76.8
      if(type .eq. 're')xnoise=-27.7*alog10(f) + 72.5
      if(type .eq. 'ru')xnoise=-27.7*alog10(f) + 67.2
      if(type .eq. 'qr')xnoise=-28.6*alog10(f) + 53.6
      if(type .eq. 'qm')xnoise=-27.5*alog10(f) + 60.0
c
c   galactic noise
c
      gnos=0.0
      if(f .ge. gnoslm) gnos=52.0-23.0*alog10(f)
c
c   add the noises(random phase approximation = add the power in watts
c
      xrnse=10.0*alog10(10.0**(atmno*0.1)+10.0**(gnos*0.1)+10.0**(xnoise
     & *0.1))
      nnum=num
c
      return
      end
```

```
      subroutine sealos (wind,freq,range,xloss)
cp
c      subroutine sealos
c
c        call sealos(wind,freq,range,xloss)
c
c        this routine calculates the additional loss (xloss) in groundwa
ve
c        propagation due to rough seas.  this routine is an empirical fi
t
c        of barrick 1970.  sealos is accurate to better than 1 db
c        between 10-50 mhz and 10-1000 km.  for frequencies greater than
 10
c        mhz it should be reasonably accurate, but for frequencies below
c        10 mhz it could be significantly in error.  the required input
c        wind velocity (wind), frequency (freq), and distance (range).
c
c        subroutines and functions used:  none
c
c        common blocks:  none
c
cz
       real n
c
c   test if freq below limits of this routine
c
      xloss=0.0
      if(freq.lt.9.0) go to 9999
c
c   pathrange of minimum loss
c
      rngmin=157.*alog10(freq) - 137.
c
      rng=amax1(rngmin,range)
c
c   calculation of the loss at 1000km. note n,c are functions of freq
c
      n= 7.2896 * freq**(-0.4477)
      c= 0.00337 * (freq-9.)**1.0047
c
      xl1000= c * wind**n
c
c   calculation of the loss at specified distance, normalized to
c   1000km.   the slope is a function of frequency
c
      if(freq .gt. 9.9) b= -0.17198*alog10(freq-9.9) + 0.61512
      if(freq .le. 9.9) b= .95908
      a=xl1000/(1000.**b)
c
      xloss= a * rng**b
c
9999  return
      end
```

APPENDIX B

BASIC SURFACE-WAVE PROGRAM

The listing of the EPM-73 APES model that follows is written in extended BASIC for the Tektronic 4052A computer.

```
2100 SUB Powerr  ! POWER(R) VER 1.0
2101       !
2102       !
2105     LOCAL H1,H2,H3,H4,H5,H6,H7,H8,H9,H,D1,D2,D3,D4,L,L4
2106       !
2110     GO TO E9 OF 2120,2220,2270,2320,2370,2420,2470,2170
2120     H2=81
2130     H3=0
2140     H4=5
2150     H5=0
2160     GO TO 2510
2170     H2=110.295
2180     H3=-0.4173
2190     H4=0.1115
2200     H5=0.10623
2210     GO TO 2510
2220     H2=110.295
2230     H3=-0.4173
2240     H4=0.1115
2250     H5=0.10623
2260     GO TO 2510
2270     H2=78.349
2280     H3=-0.4586
2290     H4=0.03547
2300     H5=0.2136
2310     GO TO 2510
2320     H2=22.142
2330     H3=-0.192
2340     H4=0.002754
2350     H5=0.459
2360     GO TO 2510
2370     H2=12.3225
2380     H3=-0.19841
2390     H4=3.419E-4
2400     H5=0.4472
2410     GO TO 2510
2420     H2=5.256
2430     H3=-0.195
2440     H4=5.3E-5
2450     H5=0.4947
2460     GO TO 2510
2470     H2=14.416
2480     H3=-0.1276
2490     H4=5.973E-4
2500     H5=0.559
2510     H8=H2*F0^H3
2520     H9=H4*F0^H5
2530     H6=300/F0*SQR(H8*H8+(60*(300/F0)*H9)^2)
2532     IF Gg1(4,25)=0 THEN   ! TEST FOR HORIZONTAL POL
2534        H6=300/F0
2536     END IF
2540     H7=2*PI*SQR(SQR((H8-1)^2+(60*(300/F0)*H9)^2))
2550     H=H6/H7*3.281
2554     IF Gg1(4,25)=0 THEN   !TEST FOR HORIZ POL
2556        H=0
```

```
2558     END IF
2560     H1=SQR(H^2+Ht^2)
2570     H2=SQR(H^2+Hr^2)
2580     D1=10^(LGT(F0)+0.75*LGT(H1*H2)-3.92)
2590     D2=129/SQR(F0)
2600     L4=33+20*LGT(F0*R)
2610     IF R<=D2 THEN 2780
2620     CALL Mfactor
2630     IF F0>40 THEN 2670
2640     REM - EQN(23)
2650     L=111-15*LGT(H1*H2)+20*LGT(D2*R)+0.62*M5*(R-D2)
2660     GO TO 2790
2670     D3=D5-48.3*LGT(F0)+163
2680     IF E9<>1 THEN 2710
2690     D4=-4*D5-1.29*F0+406
2700     D3=D3 MAX D4
2710     IF R>D3 THEN 2750
2720     REM - EQN(23)
2730     L=111-15*LGT(H1*H2)+20*LGT(D2*R)+0.62*M5*(R-D2)
2740     GO TO 2790
2750     REM - EQN(24)
2760     L=111-15*LGT(H1*H2)+40*LGT(R)+20*LGT(D2/D3)+0.62*M5*(D3-D2)
2770     GO TO 2790
2780     L=111-15*LGT(H1*H2)+40*LGT(R)
2790     L=L MAX L4+5
2800     REM QUASI MINIMUM NOISE + 14 DB MISC LOSS
2810     P=L+B+S+X9-130
2820     J=INT(F0)-1
2830     J=J MAX 2 MIN 29
2832     IF J=>21 THEN
2834        J=INT((J-20)/2)+20
2836     END IF
2840       !CALL Antfilt
2850     CALL Anteff
2858     A8=Gg1(1,J)+E6  !6 DEG TAKE OFF ANGEL USED FOR GND WAVE
2860     P=P-A8
2870 END SUB
2880 SUB Mfactor
2885     IF Gg1(4,25)=0 THEN 2910  ! TEST FOR HORIZONTAL POLARIZATION
2890     IF F0<=10 THEN 2950
2900     IF E9=1 THEN 2930
2910     M5=F0^(1/3)/7
2920     GO TO 3020
2930     M5=LGT(F0)/2-0.35
2940     GO TO 3020
2950     IF E9=1 THEN 3010
2960     IF E9=2 OR E9=8 THEN 2990
2970     M5=F0^(1/3)/7
2980     GO TO 3020
2990     M5=LGT(F0)/4+0.06
3000     GO TO 3020
3010     M5=SQR(F0)/20
3020     M5=M5 MIN 0.5
3030 END SUB
```

APPENDIX C

A STUDY OF EFFECTS OF

SURFACE REFRACTIVITY ON GROUND-WAVE PROPAGATION

C.1. INTRODUCTION

In 1977 Hanson reported the results of experimental measurements made on a 235 km over-ocean southern California path (Hansen, 1977). Stepped frequency soundings were taken twice per day for a one month period and hourly for one 24-hour period. In general the data compared well with theoretical calculations of basic ground-wave transmission loss, including the effect of varying sea state. At frequencies above 20 MHz, the measured signal levels were considerably above those expected on the basis of ground-wave theory. At 32 MHz, the measured signal levels were at times 25 dB greater than predicted. Pappert and Goodhart (1979), using calculations involving standard waveguide theory along with available radiosonde data, showed that this signal enhancement observed on frequencies above 20 MHz was due to superrefractive environments. They also showed that an exceptionally strong inversion layer was not necessary to produce significant enhanced signals.

In an attempt to determine how predicted ground-wave transmission loss is affected by realistic environments, the ground-wave program GWSNR2 was run for the same environments and paths studied by Pappert and Goodhart (1979). GWSNR2 accounts for atmospheric refraction by assuming an effective earth radius which is k times the actual earth's radius. The average and standard deviation of the refractivity gradient at 1 km for the same nine profiles as were used by Pappert and Goodhart (1979) to find the average, upper, and lower one-sigma effective earth radii. These three radii were then used to calculate the transmission loss for the path measured by Hansen (1977). Calculations were made for sea states 0, 1, and 2.

C.2. GWSNR2

GWSNR2 is a ground-wave propagation prediction program based on GWSNR developed by Berry (1978). In addition to calculating the basic transmission loss, GWSNR2 determines the signal-to-noise ratio and circuit reliability for a ground-wave path. GWSNR2 also includes Barricks' (1970, 1971a, and 1971b) sea-state surface impedance.

GWSNR solves the integral for field strength above a special earth. The program selects one of three techniques for solving the integral, depending on whether the observation point is clearly visible to the source, in the penumbra, or in the deep shadow. In the visible region, a saddle-point evaluation is employed. In the penumbra, the computer does a complex numerical integration around a contour enclosing the poles of the integrand. In the deep shadow region, the residue series is used; it involves Fock's forms of the Airy functions and their roots. The computer output has been checked by Berry (1978) against Norton's (1936, 1937a, 1937b, 1941, and 1957) curves and also against the known solutions in the visible region, and the results agree.

C.3 TROPOSPHERIC ENVIRONMENT

Pappert and Goodhart (1979) used nine tropospheric environments for their calculations. These environments were the altitude versus modified refractivity plots for Point Loma (PL), Point Mugu (PM), Montgomery Field (MF), and San Nicolas Island (SN) soundings.

To determine the effective earth's radius the following procedure was followed. Using the relationship between the modified refractivity M and radio refractivity N,

$$M(h) = N(h) + \frac{h}{a} 10^6 , \qquad \text{(C-1)}$$

the relationship between the gradients dM/dh and dN/dh was found to be

$$\frac{dN}{dh} = \frac{dM}{dh} - \frac{10^6}{a} = \frac{dM}{dh} - 156.99 \qquad \text{(C-2)}$$

where h is the height and a is the earth's radius in km. Using 6373 km as the earth's radius, the effective earth's factor k is given by

$$k = \frac{1}{1 + \frac{6373}{1 + N \times 10^{-6}} \frac{dN}{dh} 10^{-6}} . \qquad \text{(C-3)}$$

Because $1 + N \times 10^{-6}$ in equation (C-3) is for all practical purposes nearly 1, k becomes

$$k = \frac{1}{1 + 6373 \frac{dN}{dh} 10^{-6}} \qquad \text{(C-4)}$$

To determine k using equations (C-2) and (C-4), it was assumed that the atmospheric refractivity N decayed linearly with height from the surface to 1 km above the surface.

The results of determining k and ΔN for each of the nine profiles is given in table C.1. The average value for ΔN was -91.01 and its standard deviation was 20.54. Using ΔN = -91.01, the average value k was found to be 2.38005. Using $\Delta N + \sigma_{\Delta N}$ and $\Delta N - \sigma_{\Delta N}$, the upper and lower one sigma points of k were found to Le 1.814995 and 3.456559.

Table C.1. Effective earth's radii factor k for environment cases

Refractivity Profile	ΔM(1 km)	ΔN(1 km)	k
PL, 6/27/74 2012Z	96.35	-60.64	1.629574
MF, 6/28/74 0000Z	106.37	-50.62	1.476025
MF, 6/28/74 1200Z	59.22	-97.77	2.651825
PM, 6/28/74 0500Z	47.58	-109.41	3.300993
SN, 6/28/74 0500Z	57.97	-99.02	2.709037
SN, 6/27/74 2200Z	54.64	-102.35	2.874232
PM, 6/27/74 1700Z	60.13	-96.86	2.611673
PM, 6/27/74 2800Z	57.19	-99.80	2.746005
PM, 6/28/74 1300Z	54.38	-102.61	2.887982

C.4. RESULTS OF GWSNR2 CALCULATIONS

Calculations of transmission loss were made using GWSNR2 for the 235-km southern California path used by Hansen (1977) for his measurements. These calculations were made for sea states 0, 1, and 2 (0-knot, 5-knot, and 10-knot winds). The results for sea state 0 are presented in figure C-1 along with Hansen's (1977) measurements for the frequency range 4 to 32 MHz. At each frequency the vertical bars represent standard deviations on each side of the average which is at the center of the appropriate bar. Also for comparison purposes the normal four-thirds earth ground-wave path loss is shown. Note the vast improvement over the four-thirds earth model above 20 MHz. Below about 20 MHz the calculations are generally higher than measured, a result expected on the basis of sea state effects. It will be observed in figure C-1 that the calculated standard deviation is considerably larger than measured likely due to lateral inhomogeneity in the atmospheric profile at any given time.

The results of the effect of sea state are shown in figure C-2. Here the predicted results using the average effective earth radius for sea states 0, 1, and 2 are shown and Hansen's (1977) average measured results. For sea state 2 the results are in closer agreement with Hansen's (1977) measured results in the frequency range 4 to 20 MHz than the zero sea state, but the results above 24 MHz are farther away. These results at the higher frequencies may be due in part to a lateral inhomogeneity in the effects of winds over the path; Barrick's (1970, 1971a, and 1971b) work assumes that the effect of winds is steady. Except in the frequency range 28 to 32 MHz, the sea state 1 conditions tend to enhance the signal strength and cause the predicted results to be further enhanced than the measured results than was sea state 0.

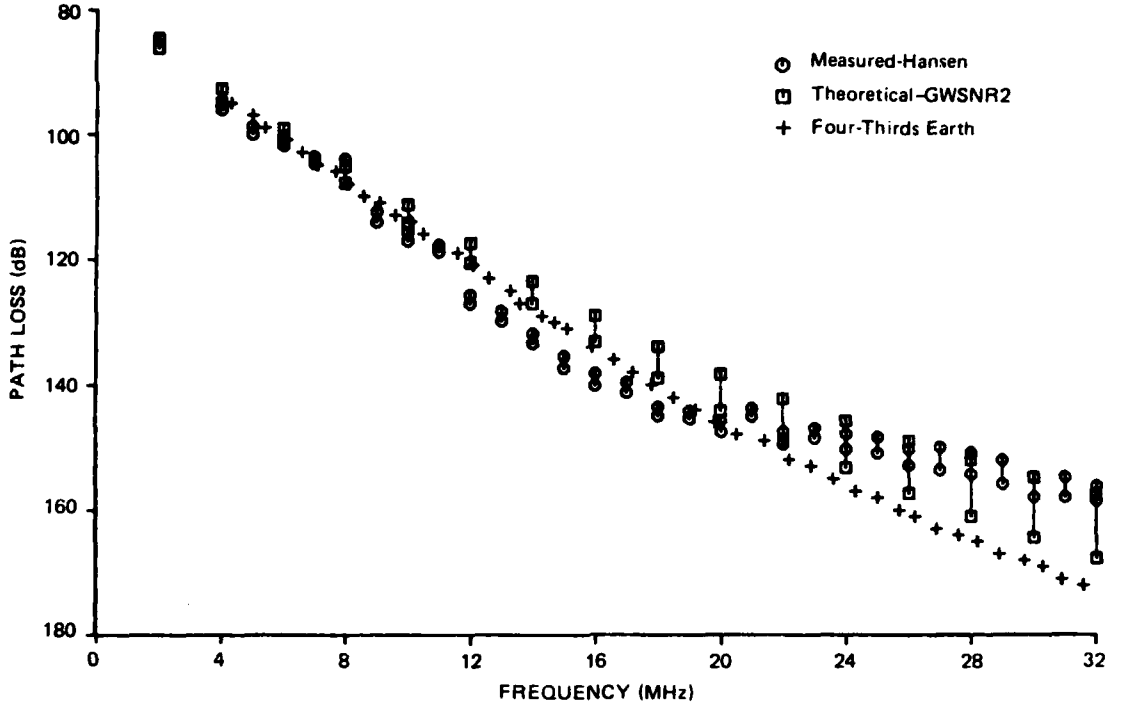

Figure C-1. Theoretical and experimental statistical over-sea loss comparison for GWSNR2 along with ground-wave results for the standard atmosphere.

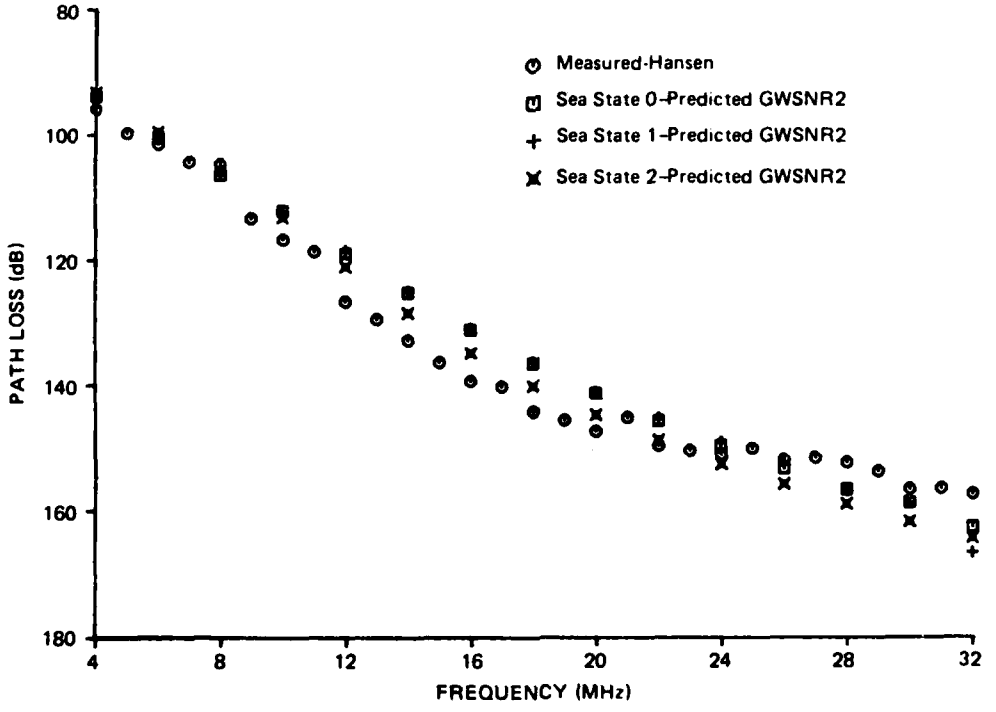

Figure C-2. Average path loss for sea states 0, 1, and 2 using GWSNR2 compared with measurement.

C.5 DISCUSSION

It has been shown that the average calculated path loss using GWSNR2, over the 4-to-32 MHz band, based on the nine environments of Pappert and Goodhart (1979), are in excellent agreement with Hansen's (1977) measured results. Disparity between the calculated and observed standard deviation can be attributed to the likelihood of lateral inhomogeneity in the atmosphere at any given time. Disparity in results at sea states greater than 0 at frequencies above 24 MHz can be attributed to the likelihood of an inhomogeneity in sea state at any given time being more noticeable above 24 MHz.

Pappert and Goodhart (1979) noted a strong inversion layer is not required to produce significant enhancements. For example they found that the PM 1700Z profile, although superrefractive, does not show a particularly strong inversion layer but yields one of the highest signal levels at the high end of the frequency band, while the PM 0500Z profile which shows a strong inversion layer yields one of the highest path losses. From table C.1, we note that profile PM 1700Z has an effective earth radius of 2.611673 and profile PM 0500Z has an effective earth radius of 3.300993. In GWSNR2 the profile PM 1700Z would show a larger transmission loss than would the profile PM 0500Z. The results here might indicate that it may be more important to specify the correct effective earth radius in ground-wave calculations. To examine this, the transmission loss should be determined using GWSNR2 for the nine individual profiles and the results compared to that of Pappert and Goodhart (1979). Further, the statistical average, upper and lower sigma values of these transmission losses should be determined and compared to Hansen's (1977) measurements. Since the average and standard deviations are based on only nine values, the confidence range in the average values should also be determined. Since the confidence in the estimated mean is $S/\sqrt{n}$ where s is the sample standard deviation and n is the number in the sample, it is possible that the disparity noted in the estimated and measured standard deviations might be due to sample size. Hansen (1977) had 36 values; whereas, Pappert and Goodhart had nine profiles. Since the estimated sample mean and standard deviation grow with increasing frequency, the confidence in the estimated mean will decrease with increasing frequency proportional to $1/\sqrt{n}$.

END

DATE

FILMED

DTIC

JULY 88